European Commission

JRC SCIENTIFIC AND POLICY REPORTS

Development of inventory datasets through remote sensing and direct observation data for earthquake loss estimation

SYNER-G Reference Report 3

Editors: Patrizia Tenerelli and Helen Crowley

Reviewers: Amir M. Kaynia

Publishing Editors: Fabio Taucer and Ufuk Hancilar

2013

Joint
Research
Centre

Europe Direct is a service to help you find answers to your questions about the European Union
Freephone number (*): 00 800 6 7 8 9 10 11
(*) Certain mobile telephone operators do not allow access to 00 800 numbers or these calls may be billed.

A great deal of additional information on the European Union is available on the Internet.
It can be accessed through the Europa server http://europa.eu/.

Printed in Ispra (Va) - Italy

D 8.9

DELIVERABLE

PROJECT INFORMATION

Project Title:	**Systemic Seismic Vulnerability and Risk Analysis for Buildings, Lifeline Networks and Infrastructures Safety Gain**
Acronym:	SYNER-G
Project N°:	244061
Call N°:	FP7-ENV-2009-1
Project start:	01 November 2009
Duration:	36 months

DELIVERABLE INFORMATION

Deliverable Title:	**D8.9 - Development of inventory datasets through remote sensing and direct observation data for earthquake loss estimation**
Date of issue:	31 March 2013
Work Package:	WP8 – Guidelines, recommendations and dissemination
Deliverable/Task Leader:	Joint Research Centre
Editors:	Patrizia Tenerelli (JRC) and Helen Crowley (UPAV)
Reviewer:	Amir M. Kaynia (NGI)

REVISION: Final

The SYNER-G Consortium

Aristotle University of Thessaloniki (Co-ordinator) (AUTH)

Vienna Consulting Engineers (VCE)

Bureau de Recherches Geologiques et Minieres (BRGM)

European Commission – Joint Research Centre (JRC)

Norwegian Geotechnical Institute (NGI)

University of Pavia (UPAV)

University of Roma "La Sapienza" (UROMA)

Middle East Technical University (METU)

Analysis and Monitoring of Environmental Risks (AMRA)

University of Karlsruhe (KIT-U)

University of Patras (UPAT)

Willis Group Holdings (WILLIS)

Mid-America Earthquake Center, University of Illinois (UILLINOIS)

Kobe University (UKOBE)

Foreword

SYNER-G is a European collaborative research project funded by European Commission (Seventh Framework Program, Theme 6: Environment) under Grant Agreement no. 244061. The primary purpose of SYNER-G is to develop an integrated methodology for the systemic seismic vulnerability and risk analysis of buildings, transportation and utility networks and critical facilities, considering for the interactions between different components and systems. The whole methodology is implemented in an open source software tool and is validated in selected case studies. The research consortium relies on the active participation of twelve entities from Europe, one from USA and one from Japan. The consortium includes partners from the consulting and the insurance industry.

SYNER-G developed an innovative methodological framework for the assessment of physical as well as socio-economic seismic vulnerability and risk at the urban/regional level. The built environment is modelled according to a detailed taxonomy, grouped into the following categories: buildings, transportation and utility networks, and critical facilities. Each category may have several types of components and systems. The framework encompasses in an integrated fashion all aspects in the chain, from hazard to the vulnerability assessment of components and systems and to the socio-economic impacts of an earthquake, accounting for all relevant uncertainties within an efficient quantitative simulation scheme, and modelling interactions between the multiple component systems.

The methodology and software tools are validated in selected sites and systems in urban and regional scale: city of Thessaloniki (Greece), city of Vienna (Austria), harbour of Thessaloniki, gas system of L'Aquila in Italy, electric power network, roadway network and hospital facility again in Italy.

The scope of the present series of Reference Reports is to document the methods, procedures, tools and applications that have been developed in SYNER-G. The reports are intended to researchers, professionals, stakeholders as well as representatives from civil protection, insurance and industry areas involved in seismic risk assessment and management.

Prof. Kyriazis Pitilakis
Aristotle University of Thessaloniki, Greece
Project Coordinator of SYNER-G

Fabio Taucer and Ufuk Hancilar
Joint Research Centre
Publishing Editors of the SYNER-G Reference Reports

Abstract

This report summarizes the lessons learnt in extracting exposure information for the three study sites, Thessaloniki, Vienna and Messina that were addressed in SYNER-G. Fine scale information on exposed elements that for SYNER-G include buildings, civil engineering works and population, is one of the variables used to quantify risk. Collecting data and creating exposure inventories is a very time-demanding job and all possible data-gathering techniques should be used to address the data shortcoming problem. This report focuses on combining direct observation and remote sensing data for the development of exposure models for seismic risk assessment. In this report a summary of the methods for collecting, processing and archiving inventory datasets is provided in Chapter 2. Chapter 3 deals with the integration of different data sources for optimum inventory datasets, whilst Chapters 4, 5 and 6 provide some case studies where combinations between direct observation and remote sensing have been used. The cities of Vienna (Austria), Thessaloniki (Greece) and Messina (Italy) have been chosen to test the proposed approaches.

Keywords: inventory data, remote sensing, direct observation, census, risk assessment

Acknowledgments

Deliverable Contributors

Joint Research Centre (JRC)	Patrizia Tenerelli	Sections 2.1.1, 2.1.2, 2.1.3, 2.1.4, 2.1.5, 2.1.6, 2.1.7, 2.1.8, 2.2.1, 2.3, 5.2, 7
	Ufuk Hancilar	
	Fabio Taucer	
	Daniele Ehrlich	
University of Pavia (UPAV)	Diego Polli	Sections 1, 2.1.9, 4.2, 6, 7
	Fabio Dell'Acqua	
	Gianni Lisini	
	Helen Crowley	
	Miriam Colombi	
Aristotle University of Thessaloniki (AUTH)	Sotiris Argyroudis	Section 5.1
	Kalliopi Kakderi	
Bureau de Recherches Geologiques et Minieres (BRGM)	Daniel Raucoules	Section 2.2.2
	Pierre Gehl	
Vienna Consulting Engineers (VCE)	Helmut Wenzel	Section 4.1
	David Schäfer	

Table of Contents

List of Figures

List of Tables

1 Introduction

Seismic disaster risk modelling requires exposure information that in SYNER-G includes the building stock, civil engineering works and population. Exposure information is rarely readily available with the characteristics required for risk modelling. Where data is available, its format, resolution and level of information are often not standardized. Furthermore, a considerable amount of fine detailed data – typically available with local authorities - are not accessible due to confidentiality issues.

Collecting data and creating exposure inventories is a time-consuming and expensive activity. Different techniques should thus be used and combined to address the data shortcoming. Depending on a number of factors such as the necessary temporal and spatial resolution, different remote sensing systems can be used to collect images and data, and different methodologies can then be implemented to manage and post-process them to develop the required inventory. Census and street survey data can be used to support and further classify data collected by remote sensing. This is of particular importance for seismic risk assessment, where a number of structural characteristics are not visible from remotely sensed images.

In this report a summary of the methods for collecting, processing and archiving inventory datasets is provided in Chapter 2. Chapter 3 deals with the integration of different data sources for the development of optimum inventory datasets, whilst Chapters 4, 5 and 6 provide some case studies where a combination of both direct observation and remote sensing has been used. The cities of Vienna (Austria), Thessaloniki (Greece) and Messina (Italy) have been chosen to test the proposed approaches.

2 Summary of methods for collecting, processing and archiving inventory datasets

2.1 REMOTE SENSING

Satellite and airborne remote sensing data may provide exposure information in a timely and cost effective manner. In fact, remote sensing data have been used in numerous case studies for spatial approaches to characterize the physical exposure and vulnerability for risk assessment (Mueller et al. 2006, Ehrlich and Tenerelli 2012).

The different types of remote sensing systems are sensitive to specific wavelengths of the electromagnetic spectrum and have different advantages and disadvantages for specific applications. Satellite and airborne remote sensing typically collect information in the Optical part of the Electro Magnetic Radiation (EMR) Spectrum and in the Radar part of the EMR spectrum. Optical sensors are sensitive to visible and infrared wavelengths; optical hyperspectral sensors, in particular, collect information in a high number of spectral bands. Radar, or SAR (Synthetic Aperture Radar), sensors use microwaves that detect the signal scattered back from objects on the ground. Optical and radar data can produce stereo models which allow for the processing of 3D surfaces.

Spatial resolution is critical for mapping physical exposure (buildings and civil engineering works). When conducting studies at the local scale, and considering a medium building size of $10m^2$, a spatial resolution of 5x5m or less is needed. Data with a minimum resolution of 1x1m are normally defined as Very High Resolution (VHR). High Resolution (HR) data are typically characterized by a spatial resolution between 1x1 and 10x10m. Medium Resolution (MR) data - with a spatial detail between 10x10 and 100x100m - can be used to detect building aggregates for larger study areas (Taubenböck et al 2012). Resolution coarser than 100 x 100 m (Low Resolution – LR) is considered for the global analysis of the built-up areas and is typically of little use for local studies.

Temporal resolution becomes relevant when a specific time scale is required and when multi-temporal analysis is needed for monitoring building stock and urban area changes. Multi-temporal data can also be exploited to detect the building age.

VHR and HR data accessibility from remote sensing largely depends on the available funding. Aerial photography, which allows for a higher spatial resolution, is more expensive than satellite data. On the other hand, satellite imagery provides a synoptic view of large areas, and a nearly global coverage is available from different data providers. Satellite data also allows for the collection of datasets with spatial resolutions that are comparable to those of aerial photography. The interest in satellite data applications for physical exposure analysis is therefore rapidly increasing.

Only the above-ground physical infrastructure, including buildings, utility networks, and transport corridors, can be observed by remote sensing. Table 2.1 lists the most suitable types of satellite imagery that can be used to gather information on the European elements at risk. Descriptions for the suggested remote sensing imagery are given in the following sections.

Table 2.1 Remote sensing data types and detectable physical parameters for each typical European element at risk

Typical European elements at risk		Visible from remote sensing	Automatic and semi-automatic detection	Physical parameter that can be identified	Suggested data types
BUILDINGS		Yes	Possible	Building location, planar view, built-up density, roof type, building age, geometrical parameters (shape, perimeter, size height, volume)	Optical VHR/HR/MR; Stereo VHR/HR; Hyper-spectral HR; Oblique Aerial; LIDAR*; SAR VHR/HR
UTILITY NETWORKS	Electric power system	Partially**	Unlikely	Location and geometric parameters of elements above the earth surface (i.e. power stations)	Optical VHR; Stereo VHR/HR; Oblique Aerial; LIDAR*
UTILITY NETWORKS	Gas and oil network	Partially**	Unlikely	Location and geometric parameters of elements above the earth surface (i.e. pipelines, tanks)	Optical VHR; Stereo VHR/HR; Oblique Aerial; LIDAR*
UTILITY NETWORKS	Water and waste-water system	Partially**	Unlikely	Location and geometric parameters of elements above the earth surface (i.e. pipelines, dams)	Optical VHR; Stereo VHR/HR; Oblique Aerial; LIDAR*; Hyper-spectral HR
TRANSPORTATION INFRASTRUCTURES	Roadway bridges	Partially**	Possible	Bridge location and width	Optical VHR; Stereo VHR/HR; SAR VHR; Oblique Aerial; LIDAR*
TRANSPORTATION INFRASTRUCTURES	Roadway system	Yes	Possible	Road main axis and width	Optical VHR; SAR VHR; Hyperspectral HR
TRANSPORTATION INFRASTRUCTURES	Railway system	Yes	Unlikely	Railway main axis and width	Optical VHR; SAR VHR; Hyperspectral HR
TRANSPORTATION INFRASTRUCTURES	Harbor elements	Partially**	Unlikely	Location and geometric parameters of harbor buildings and cranes	Optical VHR; Stereo VHR/HR; Oblique Aerial; LIDAR*

Typical European elements at risk		Visible from remote sensing	Automatic and semi-automatic detection	Physical parameter that can be identified	Suggested data types
CRITICAL FACILITIES	Health-care facilities	Partially**	Unlikely	Location and geometric parameters of facility buildings	Optical VHR; Stereo VHR/HR; Oblique Aerial; LIDAR*
	Fire-fighting system	Partially**	Unlikely	Location and geometric parameters of facility buildings	Optical VHR; Stereo VHR/HR; Oblique Aerial; LIDAR*

*LIDAR=Laser Imaging Detection and Ranging

** secondary information are necessary

2.1.1 Very High Resolution optical

Optical satellites measure the amount of Electromagnetic Radiation which reaches the sensor after being reflected by the earth's surface. Satellite data with a minimum resolution of 1x1m (i.e. GeoEye, WorldView, Quickbird, Ikonos, Kompsat, OrbView3) are normally defined as Very High Resolution data (VHR) and represent the most promising sources of information to derive elements of urban landscape from satellites.

VHR data are suitable for a building-by-building representation of the built-up environment. The buildings can be mapped as points or footprints (building base area). A limited number of building parameters, such as building planar view (footprint), density, height and volume, can also be derived from VHR satellite imageries. Building use (residential, commercial, industrial, etc.) can be inferred, with a certain approximation, by visual interpretation of VHR data. The building age can also be estimated from multi-temporal data analysis; however, this application is limited by the temporal resolution of available VHR data (the first publically available VHR satellite images, from IKONOS satellite, are from 1999).

Building parameters can be derived from VHR satellite imageries through computer-aided visual interpretation (photo-interpretation) or automatic classification algorithms. Automatic building parameters extraction can be a very valuable source of information when conducting large-scale analysis and when no other local dataset is available. Automatically derived information is typically less reliable than that derived from ground survey or photo-interpretation. Building parameters can be statistically aggregated to blocks/census unit or grid cells at appropriate scales. Nolte et al. (2011) and Dell'Acqua et al. (2011) provide a comprehensive overview of existing approaches and techniques to extract building parameters from VHR optical satellite imagery through automatic or semi-automatic approaches.

Several VHR satellite data types are available and can be applied to building information extraction. The choice of specific data types involves trade-off between several parameters. The trade-off is driven by the intended application. In addition to spatial resolution, also spectral resolution, viewing angle, illumination angle and atmospheric condition, should be

considered when selecting a satellite image for a specific purpose and processing technique. Some of these parameters may influence the quality of the imagery (i.e. atmospheric conditions) and thus the precision of object extraction, while some other parameters can determine the possibility to extract specific parameters - i.e. the acquisition angle and sun elevation angle influence the shadow and the view angle of high objects, which are exploited to extract buildings and object height.

Critical facilities (i.e. fire stations, dams and water supply facilities) and some above ground elements belonging to utility networks (i.e. pipelines, power stations, tanks), can be manually extracted, with a certain approximation, by visual interpretation of VHR data.

VHR data can also be applied to extract transportation infrastructures (roads, railways and bridges). An overview of existing techniques to extract transportation infrastructures from optical remote sensing can be found in Nolte et al. (2011).

2.1.2 Stereo High and Very High Resolution (i.e. aerial, satellite)

Stereo products consist of two images of the same location on Earth, taken at two different angles, which can be processed to obtain 3D surface models. Stereo HR and VHR imagery can be processed to generate very valuable building stock information, such as planar and height attributes of buildings. The precision of the measurement depends on the resolution of the input imagery and the type of processing.

Typically, stereo images are processed using photogrammetric stations with procedures that are not automated. Newly available software allow imagery to be processed in an automatic way which is, however, more prone to error. Stereo imagery's first output, the Digital Surface Model (DSM), can be refined based on ancillary information- i.e. street level elevation - to obtain a Digital Elevation model (DEM) and extract building heights. References related to DSM footprint extraction from VHR imagery include Toutin (2004a, 2004b, 2006a, 2006b) and Poli et al. (2010).

VHR Stereo imagery is among the best suited data to address the typical European elements at risk. Stereo aerial photography has been collected for decades to provide fine scale information on the built environment. Most of the VHR satellites can also acquire stereo pair imageries, with a resolution which is about two to three times lower than normal sensor acquisition. Satellite-based stereo imagery is, however, often limited by imaging angles that may not always be adequate for 3D processing.

2.1.3 Hyperspectral

Hyperspectral Imagery (HSI), or Imaging Spectrometry data, measure the Electromagnetic Radiation reflected by the earth's surface in a very high number of spectral bands (more than 200 bands), providing a contiguous spectral coverage over selected spectral ranges. Detailed spectral information can be exploited to detect Earth-surface minerals and to characterize surface materials. Spectrometers are generally transported on aerial platforms that also allow high spatial ground resolution (few meters).

Different airborne Hyperspectral data have been used for urban application, i.e. Airborne Visible InfraRed Imaging Spectrometer (AVIRIS), Multispectral Infrared and Visible Imaging Spectrometer (MIVIS), Digital Airborne Imaging Spectrometer (DAIS) and Reflective Optics System Imaging Spectrometer (ROSIS). The applications include the detection of roof

materials (brick, metallic, gravel, asphalt, shingles, tiles, wood and roof tops covered by toxic material, e.g. asbestos), urban land cover classes and sealing materials such as asphalt, bitumen, parking special cover, gravel and concrete (Herold et al. 2003, Dell'Acqua et al. 2005, Marino et al. 2001). The roof material can be used to infer, with a certain approximation, the building type. The sealing material classification can also be used to extract roadways, railways and built-up area.

2.1.4   High Resolution optical

Data from optical High Resolution (HR) satellites (i.e. SPOT, Formosat, ALOS, CBERS, RapidEye) are typically characterized by a spatial resolution ranging between 1x1m and 10x10m (Taubenböck et al 2012). HR data can be used to derive built-up binary masks (maps of built-up/non built-up) or built-up density maps. The built-up map represents buildings in spatial units with a variable area corresponding to building aggregates. The resolution of HR data does not normally allow mapping the planar view of single buildings.

Built-up maps are typically extracted through automatic or semi-automatic algorithms and can be used to approximate information on physical elements exposed to risk. Different classification procedures can be based on statistical or logical decision rules in the multispectral or spatial domain - the spatial domain includes shape, size, texture, and patterns of pixels or group of pixels - (Gao 2009). Nolte et al. (2011) and Dell'Acqua et al. (2011) provide a comprehensive overview of existing techniques to extract built-up areas applying different image classification algorithms.

Built-up maps are particularly useful to rapidly cover large areas, such as country level mapping.

2.1.5   Medium Resolution optical

Medium Resolution (MR) satellite imagery has a spatial resolution between 10x10m and 100x100m (Taubenböck et al 2012) and includes what is typically referred to as imagery collected for environmental purposes. Such datum allows built-up areas to be identified but is not able to resolve single elements of an urban landscape – building units and civil engineering works.

Large volume archives of MR satellite data covering the globe between 1982 and 2000 are now available. The data are available mostly free of charge. One of the richest repositories is that of Landsat imagery available from NASA. Landsat data has been, by and large, used to analyse environmental issues in urban settings or to map "urban" type of classes in national and continental land cover products. The most notable products are the CORINE Land Cover (EEA 1999), Afri-Cover and the North America Landscape Characterization (Vogelmann 2001). Landsat data has found large application for hydrological studies where the urban areas are outlined to identify impervious or artificial surfaces, and the heat island effect of cities.

MR data is not suited to characterize single units of the European elements at risk; the spatial resolution is just not sufficient to resolve such elements.

2.1.6 Low Resolution optical

One set of environmental satellites image the entire Earth every day at coarse resolution (100x100m or coarser). Yet, this imagery has been used to derive global land cover products which include one or more "urban" classes. Few of these global datasets have been actually validated. When urban classes are compared across land-cover datasets, discrepancies have resulted largely due to a non-standardized semantic (Potere et al. 2009).

The MODIS-Urban layer (Schnedier et al. 2009) maps major urban agglomerations with a resolution of 500x500m. This product has been validated, displaying unexpected consistency across continents.

Global scale built-up layers may not be of use in a local application such as that addressed in SYNER-G; in fact its use lies largely across regional comparison and continental to global land cover applications.

2.1.7 Oblique Aerial Imagery

Oblique Aerial data provide VHR Imagery from multiple angles with oblique perspectives. For example, Pictometry technology acquires images simultaneously from an aircraft at 40° angles (North, South, East, West and vertical) for every feature within the urban environment. Thanks to the oblique views, some specific parameters of buildings, infrastructures and facilities, that would be normally collected from ground survey, can be extracted - i.e. existence of soft stories, added attic spaces, openings and façade elements. Moreover, ground elevations, building heights, roof height and shape can be extracted with high resolution.

Oblique Aerial Imagery is among the best-suited data to address the typical European elements at risk.

2.1.8 LIDAR

LASER (Light Amplification by Stimulated Emission of Radiation) systems represent a source of high-accuracy elevation data. The LASER technology is also known as LIDAR (Laser Imaging Detection and Ranging), LADAR (LAser Detection And Ranging) or Laser Radar. LASER scanners can be mounted on an aircraft platform and applied for measurements of surface elevation profiles with sub-meter accuracy, at reduced cost compared to traditional survey methods. These measures are relevant for collecting the height and other geometric parameters of building and civil engineering works such as bridges, power lines, pipelines and dams.

2.1.9 RADAR

Synthetic Aperture Radar (SAR) systems emit radio waves and detect the signal that is scattered back from objects on the ground. The advantages of SAR compared to optical systems are that they can collect information through dense cloud cover, and they can directly provide precise information on ground elevation. The measurement of elevation is useful for terrain modelling, an important task for many hazard applications, and for monitoring changes in land surface, for example, from subsidence or landslides.

SAR sensors had been considered as unsuitable for precise characterization of the urban environment. This however has now changed. In fact the availability of VHR SAR imagery from TerraSAR-X and COSMO-SkyMed provides new data to exploit the fine scale spatial patterns characterized by human settlements (Dell'Acqua et al. 2008).

SAR data processing requires specialized training in image processing. The datum cannot intuitively be analysed as optical datum. In addition, since the signal records the dialectric properties of objects, the datum cannot uniquely be converted in a categorical class associated to an urban object. At present, a huge repository of fine resolution COSMO-SkyMed and TerraSAR-X is being built and disclosed to the research community. SAR has shown to be suitable for detecting settlements and roads and is very efficient in monitoring earth displacements when a number of images covering the same area can be processed with interferometry techniques. SAR may also be used for damage assessment, in combination with other data (Dell'Acqua et al. 2011). However, comprehensive and validated products are still not available.

Image classification software can extract features from both optical and SAR images using automatic or semi-automatic algorithms. Building height, number of storeys, footprint dimension and roads can also be extracted using a linear feature extractor, such as W-Filter, which is part of in-house developed feature extraction software named BREC (Gamba et al. 2009). An example of road extraction from a radar image is illustrated in Fig. 2.1.
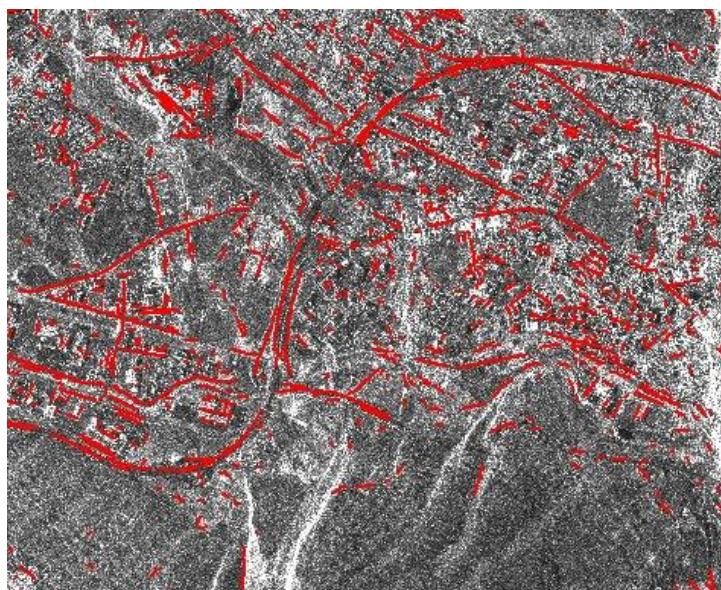
Fig. 2.1 Extraction of a road network with rapid mapping procedure from SAR data

2.2   CENSUS DATA

Census data record information on population and housing. The information is available as statistical aggregations at the level of administrative units. Censuses can also include other socio-economic parameters, such as health, crime, economic activities, labour market, education and culture. The following paragraphs describe demographic and housing census data which represent fundamental inputs in datasets for exposure and vulnerability assessment.

2.2.1 Demographic data

Population data at sub-national level are normally collected in Europe through population census every 5 to 10 years. Census units have a spatial dimension which commonly corresponds to building aggregates matching administrative districts at different scales (i.e. Nomenclature of Territorial Units for Statistics – NUTS - regions). In many cases census data are only available at the commune level. In some cases demographic and socio-economic census are conducted using grid cell spatial units. Grid-based representations of population offer several advantages when population data must be integrated with a representation of settlements or environmental phenomena (Martin 2009). More precise demographic data are collected in local administrative offices, but are normally not accessible or not available as geo-referenced digital data format.

When studying exposure, the spatial detail of elements exposed to risk affects the scale of analysis and allows scenarios to be performed with different levels of approximation. The census spatial units therefore affect the detail at which the information on human exposure can be provided. When it is not possible to collect ad hoc demographic data from the field, downscaling or spatial disaggregation techniques can be used to address heterogeneity within census units, displacing the population density to smaller and more homogeneous spatial units. The disaggregation techniques may be based on ancillary data which are normally related to the land use.

Downscaling techniques can map three types of population distribution: residential, ambient and time-specific. Time-specific and ambient population maps are based on spatio-temporal models, which take into account the movements of population during different times of the day, through a given area (Martin 2009, Ahola et al. 2007). Ambient population refers to an average distribution of population over 24 hours (Dobson et al. 2000). When mapping ambient or temporal distribution of the population, the input data collection is much more challenging. Two datasets are in fact needed in this case: the map of the activity location, or physical features where they take place, and the census of the mobile population, which include statistics on tourism, all work related travels, temporary accommodations, education and traffic (Bhaduri 2007, Martin 2009, Ahola et al. 2007).

Some population distribution maps have already been produced in Europe. A European dataset of residential population density (Population density grid of EU-27+) has been produced by the Joint Research Centre (Gallego, 2010) using a dasymetric model. The last version of this product is based on a population dataset at municipality level for the reference year of 2006, and on the Corine Land Cover map (2006 v.13) as ancillary dataset. The map represents population density as inhabitants per square kilometre with a spatial resolution of 100 m (Fig. 2.2). At the moment this population density grid is the only open source map of population density at European scale. The level of detail of this map is not sufficient to support risk assessment at the local level, in fact it is not intended to derive precise details at the city or sub-city level. However, a refined version of this European population map is being implemented based on the incorporation of some land use/land cover maps with higher resolution, such as the Soil Sealing, Urban Atlas, Tele Atlas and SRTM Water Bodies Data (Batista et al. 2012).

Population census data can also include the classification of population by sex, age, health and education, which is needed for socio-economic vulnerability analysis (Khazai et al. 2011). Those data are available for Europe at the sub-city district level from EUROSTAT through the European Urban Audit (EUA) (http://epp.eurostat.ec.europa.eu) since 2003.
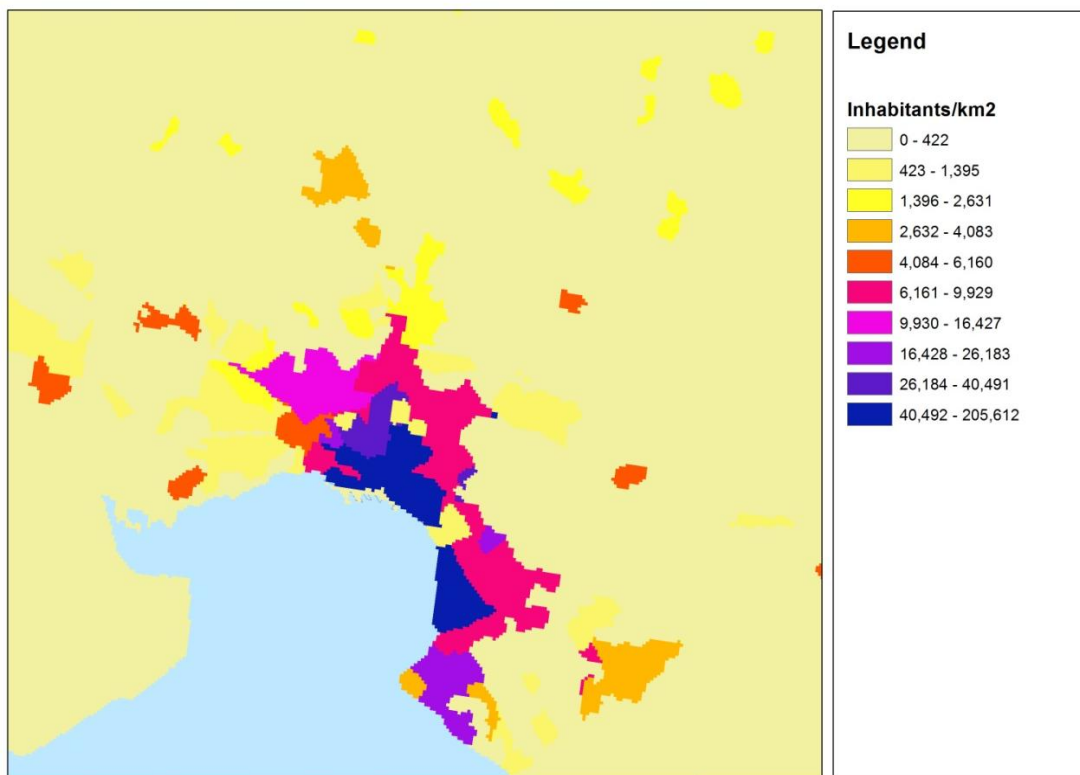
Fig. 2.2 Population density grid of EU-27+ for the city of Thessaloniki

2.2.2   Housing census data

Housing census data record the characteristics of housing for the entire population and entire geographic extent of a country. Although the level of detail and procedures involved in compiling such information is quite exhaustive, the housing census surveys are not intended for database development in earthquake loss estimation studies. The housing census compilations are commonly not carried out by engineering professionals and hence the data provide only a limited contribution for the engineering characterization of building construction types. The housing types might be deduced from the material used for constructing the roof, floors, and external walls and by the help of photos, if available, as it has been done in the compilation of the PAGER database (Jaiswal and Wald 2008). In the 2000 census (1995-2004 decade), about 173 countries conducted housing censuses. Still, many countries in the world either have not planned to conduct housing census or have not shared the information with the United Nations Statistics Division. Among the 131 countries for which the housing census data were available at the United Nations office, only 73 countries have data related to the construction material of the outer walls of buildings (Jaiswal and Wald 2008).

The EUA (http://www.urbanaudit.org/) provides European urban statistics for 258 cities across 27 European countries. It contains almost 300 statistical indicators presenting information on matters such as demography, society, economy, environment, transport, information society and leisure. The EUA was conducted at the initiative of the Directorate-General for Regional Policy at the European Commission, in cooperation with EUROSTAT and the national statistical offices of the 25 Member States at the time plus Bulgaria and Romania. EUROSTAT adopts a classification on the basis of the provisional Central Product

Classification (CPC) published in 1991 by the United Nations and considers two main categories of constructions: "Buildings" and "Civil engineering works" (Eurostat 1997). Classification of types of constructions (CC) distinguishes between technical design, which results from the special use of the structure (e.g. commercial buildings, road structures, waterworks, pipelines), from the main use of a building (e.g. residential, non-residential). If less than half of the overall useful floor area is used for residential purposes, the building is classified under non-residential buildings in accordance with its purpose-oriented design. If at least half of the overall useful floor area is used for residential purposes, the building is classified as residential. Civil engineering works include all constructions not classified under buildings: railways, roads, bridges, highways, airport runways, dams, etc. Civil engineering works are classified mainly according to the engineering design which is determined by the purpose of the structure. Residential building stock is further divided into three classes: one-dwelling buildings, two- and more dwelling buildings and residences for communities. Single-family houses include individual houses that are inhabited by one or two families including terraced houses. Multi-family houses contain more than two dwellings in the house, up to 9 storeys. High-rise buildings are defined as buildings that are higher than 8 storeys. A special building type, corresponding to panelised structure buildings, is found in most Eastern European countries. In literature and statistics, these buildings are considered as being high-rise or multi-family buildings. In the EU-25, 34 million dwellings, or 17% of the whole building stock, are panelised buildings. In each country where these buildings exist, one to three different building types are defined.

At national scale, within Europe, each national Statistical Data Institute has its own table format, linked to different methods for information collection. Table 2.1 presents the kind of data concerning the building stock which can be found in four European countries.

More detailed data is found in cadastral plans. Differently from census data, cadastral data is taken individually for each construction. This data is not always distributed by authorities because it often contains confidential information. Attributes usually included in these databases are: wall and roof material, age of construction, conservation state, number of floors, and number of households per building.

Finally, other data sources are provided by some databases based on Geographical Information System (GIS) which contain building delimitations (footprints) and some geometrical characteristics (height, surface). However, information about construction type or age is not always provided. These databases sometimes delimit building aggregates and not individual buildings.

The SYNER-G methodology accounts for the type and format of information in the available databases (Franchin et al 2011). Socio-economic data, as well as data on building type and distribution for European cities which are available from EUROSTAT, respectively, through the EUA and the Building Census (BC), are used. Data on land use are available on a local basis in the form of a Land Use Plan (LUP), usually maintained from a local source (e.g. the Municipality). However, each of these data sources adopts a different meshing of the urban territory, according to its own criteria. For example, the urban territory is subdivided in the EUA into sub-city districts (SCD), which are areas sufficiently homogeneous in terms of some socio-economic indicators (e.g. income). On the other hand the Land Use Plan, by its very nature, subdivides the territory in areas that are homogenous per use type (green, industrial, commercial, residential).

Table 2.1 Comparison of the type of data available from the respective national Statistical Databases in four European countries

Country	Dwellings or buildings	Age of construction	Number of floors	Material	Building use
France	Number of dwellings	4 periods	No	No	Dwellings in individual housing or collective
Italy	Number of buildings and dwellings	9 periods	Yes	Masonry and RC	-
Greece	Number of buildings	11 classes	Yes	7 classes of material	Residential and other uses (industrial, commercial, etc.)
Spain	Number of dwellings and buildings	9 periods	Yes	No. Information about conservation state	Residential

2.3   GROUND SURVEYS AND FIELD DATA

Ground screening procedures consist of collecting the attributes on a building-by-building basis through direct observations and street surveys and are in general used to collect data in well delimited regions. These procedures may be divided into two groups: (1) Paper forms that allow recording a number of attributes of buildings, and (2) Hand-held equipment and software that enables user-defined electronic inventory data. Building attributes may be collected either by street-front direct visual observation and/or by interpretation of street front photographs.

2.3.1   Paper forms

A joint working group of the National Seismic Survey (SSN) and the National Group for the Defence against Earthquakes (GNDT) developed a specific tool (AeDES) for damage assessment, short term countermeasures for damage limitation and evaluation of the post-earthquake usability of ordinary buildings (Baggio et al. 2007). The form is the outcome of the field experience, matured after several past earthquakes, when forms with different levels of detail were used (Irpinia '80, Abruzzo '84, Basilicata '90, Reggio Emilia '96). The AeDES survey form (Fig. 2.3) was optimised in order to limit the time required for each inspection. It collects the information needed for an expert judgement on usability, based on as objective as possible data on vulnerability and damage. Buildings are interpreted as structural units of ordinary constructional typology (i.e. masonry, reinforced concrete or steel), used for habitation and/or services. Therefore, the application of this form to buildings of very particular structural typologies (industrial warehouses, sport structures, theatres,

churches etc.), or to monuments, is excluded. The form allows a quick survey and a first identification of the building stock, with the collection of metrical and typological data of the buildings.

Another example of detailed paper forms for recording building attributes is provided by FEMA 154 - "Rapid visual screening of buildings for potential seismic hazards: A handbook". The rapid visual screening (RVS) procedure uses a methodology based on a 'sidewalk survey' of a building and a Data Collection Form, which is completed by the person conducting the survey (the screener), based on visual observation of the building from the exterior, and if possible, the interior (FEMA 2002). The Data Collection Form includes space for documenting information on the building identification, including its use and size, a photograph of the building, sketches, and documentation of pertinent data related to seismic performance, including the development of a numeric seismic hazard score (Fig. 2.4). Completion of the Data Collection Form starts by identifying the primary structural lateral-load-resisting system and structural materials of the building. Basic Structural Hazard Scores for various building types are provided on the form where the screener circles the appropriate one. For many buildings, viewed only from the exterior, this important decision requires the screener to be trained and experienced in building construction and design. The screener modifies the Basic Structural Hazard Score by identifying and circling Score Modifiers related to observed performance attributes, which are then added (or subtracted) to the Basic Structural Hazard Score to get a final Structural Score (S). The Basic Structural Hazard Score, Score Modifiers, and final Structural Score are all related to the probability of building collapse should severe ground shaking occur (that is, a ground shaking level equivalent to that currently used in the seismic design of new buildings). Final S scores typically range from 0 to 7, with higher S scores corresponding to better expected seismic performance.

SECTION 7 Soil and Foundation

SITE MORPHOLOGY	DAMAGE (present or possible): ☐ Slopes ☐ Foundation Soil
1 ○ Crest 2 ○ Steep slope 3 ○ Mild slope 4 ○ Plain	A ○ Absent B ○ Produced by eqk. C ○ Worsened D ○ Preexistent

Province Istat | | | | Municipality Istat | Team |__|__| Form No.|__|__|__|__|__|__| Date |__|__|__|__|__|__|

SECTION 8 Usability assessment

Risk evaluation

RISK	STRUCTURAL (Sect 3 e 4)
LOW	○
LOW WITH COUNTERMEASURES	○
HIGH	○

(1) Restrictions on building use

Survey accuracy
1 ○ Co...
2 ○ Pa...
3 ○ Co...

Masonry buildings

Vertical structures / Horizontal Structures	Unknown	Irregular layout or bad quality (rubble stones, pebbles,...)		Regular layout and good quality (Blocks, bricks, squared stone..)		Isolated columns	Mixed	Strengthened
		W/O tie rods or tie beams	With ties rods or tie beams	W/O tie rods or tie beams	With tie rods or tie beams			
	A	B	C	D	E	F	G	H
1 Not identified	○	☐	☐	☐	☐	SI	☐	☐
2 Vaults without tie rods	☐	☐	☐	☐	☐	○	G1	H1
3 Vaults with tie rods	☐	☐	☐	☐	☐		☐	☐
4 Beams with flexible slab (wooden beams with a single layer of wooden planks, beams and shallow arch vaults,...)	☐	☐	☐	☐	☐	NO	G2	H2
5 Beams with semirigid slab (wooden beams with a double layer of wooden planks, beams and hollow flat blocks,...)	☐	☐	☐	☐	☐	○	☐	☐
6 Beams with rigid slab (r.c. floors, beams well connected to r.c. slabs,...)	☐	☐	☐	☐	☐		G3	H3

Other structures

R.c. frames	☐
R.c. shear walls	☐
Steel frames	☐

REGULARITY	Irregular A	Regular B
1 Plan and elevation	○	○
2 Infills distribution	○	○

Roof
1 ○ Thrusting heavy
2 ○ Non thrusting heavy
3 ○ Thrusting light
4 ○ Non thrusting light

Suggested short term counterm...

	*	**	Suggested short ter...
1	☐	☐	Tightening and app...
2	☐	☐	Repair of light dam...
3	☐	☐	Roof repair
4	☐	☐	Stairs propping
5	☐	☐	Removal of plaster
6	☐	☐	Removal of tiles, c...

Unusable building units, famili...

Unusable building units |__|

SECTION 9 Notes

On damage, short term counter...

Topic

The su...

SECTION 4 Damage to structural elemen...

Structural component / Pre-existing damage	Damage level - extension DAMA...				
	D4-D5 Very Heavy			D2-D3 Medium-Se...	
	>2/3 A	1/3 - 2/3 B	<1/3 C	>2/3 D	1/3 - 2/3 E
1 Vertical structures	☐	☐	☐	☐	☐
2 Floors	☐	☐	☐	☐	☐
3 Stairs	☐	☐	☐	☐	☐
4 Roof	☐	☐	☐	☐	☐
5 Infills and partitions	☐	☐	☐	☐	☐
6 Pre-existing damage	☐	☐	☐	☐	☐

(1) - The damage extension must be filled only if the correspon...

SECTION 5 Damage to non-structural el...

Damage	PRESENT A
1 Falling of plaster, coverings, false-ceilings	○
2 Falling of tiles, chimneys...	○
3 Falling of eaves, parapets,...	○
4 Falling of other internal or external objects	○
5 Damage to hydraulic or sewage systems	○
6 Damage to electric or gas systems	○

SECTION 6 External risk induced by oth...

Potential cause	Building A
1 Objects falling from adjacent buildings	☐
2 Failure of distribution systems	☐

SECTION 1 Building identification

Province:
Municipality:
Locality:

Team |__|__|__| Form n |__|__|__|__| day month year
Date |__|__|__|__|__|__|

1.1. BUILDING IDENTIFICATION

Region Istat | Province Istat | Municipality Istat | Aggregate No. | Building No.

Istat Hamlet code |__|__|__| Type of map
Istat Census code |__|__|__| Map No. |__|__|__|__|
Cadastral data Sheet |__|__|__| Allegato |__|__|
Parcels |__|__|__|__|__|__|__|__|

Address
1 ○ Street
2 ○ Road
3 ○ Alley
4 ○ Square
5 ○ Other

Number | | | | |

Building position 1 ○ Isolated 2 ○ Internal 3 ○ Extreme 4 ○ Corner

Building denomination or owner's name |__|__|__|__|__|__|__|__|__|__|__| Destination Code |S|__|__|

Photocopy of the structural aggregate with building indication

SECTION 2 Building description

Total number of stories	Average storey height [m]	Average storey surface [m²]		Construction and renovation [max 2]	Use	No. of units in use	Utilisation	No. of occupants 100 10 1
○ 1 ○ 9	1 ○ ≤ 2.50	A ○ ≤ 50	I ○ 400÷500	1 ○ ≤ 1919	A ○ Residential	|__|	A ○ > 65%	0 0 0
○ 2 ○ 10	2 ○ 2.50÷3.50	B ○ 50÷70	L ○ 500÷650	2 ○ 19÷45	B ○ Production	|__|	B ○ 30÷65%	1 1 1
○ 3 ○ 11	3 ○ 3.50÷5.0	C ○ 70÷100	M ○ 650÷900	3 ○ 46÷61	C ○ Business	|__|	C ○ < 30%	2 2 2
○ 4 ○ 12	4 ○ > 5.0	D ○ 100÷130	N ○ 900÷1200	4 ○ 62÷71	D ○ Offices	|__|	D ○ Not utilised	3 3 3
○ 5 ○ >12		E ○ 130÷170	O ○ 1200÷1600	5 ○ 72÷81	E ○ Public services	|__|	E ○ In construction	4 4 4
○ 6	No. of basements	F ○ 170÷230	P ○ 1600÷2200	6 ○ 82÷91	F ○ Warehouse	|__|	F ○ Uncompleted	5 5 5
○ 7	A ○ 0 C ○ 2	G ○ 230÷300	Q ○ 2200÷3000	7 ○ 92÷01	G ○ Strategic services	|__|	G ○ Abandoned	6 6 6
○ 8	B ○ 1 D ○ ≥3	H ○ 300÷400	R ○ >3000	8 ○ ≥ 2002	H ○ Touristic	|__|	Property A ○ Public	7 7 7 / 8 8 8 / 9 9 9

B ○ Private

SECTION 3 Building Typology (multiple answer; for masonry buildings indicate max 2 combinations of vertical and horizontal structures)

Fig. 2.3 AeDES survey form (Baggio et al. 2007)

LOW

Rapid Visual Screening of Buildings for Potential Seismic Hazards
FEMA-154 Data Collection Form

LOW Seismicity

Address: _____
_____ Zip _____
Other Identifiers _____
No. Stories _____ Year Built _____
Screener _____ Date

MODERATE

Rapid Visual Screening of Buildings for Potential Seismic Hazards
FEMA-154 Data Collection Form

MODERATE Seismicity

Address: _____
_____ Zip _____
Other Identifiers _____
No. Stories _____ Year Built _____
Screener _____ Date

HIGH

Rapid Visual Screening of Buildings for Potential Seismic Hazards
FEMA-154 Data Collection Form

HIGH Seismicity

Address: _____
_____ Zip _____
Other Identifiers _____
No. Stories _____ Year Built _____
Screener _____ Date _____
Total Floor Area (sq. ft.) _____
Building Name _____
Use _____

PHOTOGRAPH

Scale:

OCCUPANCY		SOIL		TYPE						FALLING HAZARDS			
Assembly Govt	Office	Number of Persons	A Hard Rock	B Avg. Rock	C Dense Soil	D Stiff Soil	E Soft Soil	F Poor Soil		Unreinforced Chimneys	Parapets	Cladding	Other:
Commercial Historic	Residential	0 – 10 11 – 100											
Emer. Services Industrial	School	101-1000 1000+											

BASIC SCORE, MODIFIERS, AND FINAL SCORE, S

BUILDING TYPE	W1	W2	S1 (MRF)	S2 (BR)	S3 (LM)	S4 (RC SW)	S5 (URM INF)	C1 (MRF)	C2 (SW)	C3 (URM INF)	PC1 (TU)	PC2	RM1 (FD)	RM2 (RD)	URM
Basic Score	4.4	3.8	2.8	3.0	3.2	2.8	2.0	2.5	2.8	1.6	2.6	2.4	2.8	2.8	1.8
Mid Rise (4 to 7 stories)	N/A	N/A	+0.2	+0.4	N/A	+0.4	+0.4	+0.4	+0.4	+0.2	N/A	+0.2	+0.4	+0.4	0.0
High Rise (> 7 stories)	N/A	N/A	+0.6	+0.8	N/A	+0.8	+0.8	+0.6	+0.8	+0.3	N/A	+0.4	N/A	+0.6	N/A
Vertical Irregularity	-2.5	-2.0	-1.0	-1.5	N/A	-1.0	-1.0	-1.5	-1.0	-1.0	N/A	-1.0	-1.0	-1.0	-1.0
Plan irregularity	-0.5	-0.5	-0.5	-0.5	-0.5	-0.5	-0.5	-0.5	-0.5	-0.5	-0.5	-0.5	-0.5	-0.5	-0.5
Pre-Code	0.0	-1.0	-1.0	-0.8	-0.6	-0.8	-0.2	-1.2	-1.0	-0.2	-0.8	-0.8	-1.0	-0.8	-0.2
Post-Benchmark	+2.4	+2.4	+1.4	+1.4	N/A	+1.6	N/A	+1.4	+2.4	N/A	+2.4	N/A	+2.8	+2.6	N/A
Soil Type C	0.0	-0.4	-0.4	-0.4	-0.4	-0.4	-0.4	-0.4	-0.4	-0.4	-0.4	-0.4	-0.4	-0.4	-0.4
Soil Type D	0.0	-0.8	-0.6	-0.6	-0.6	-0.6	-0.4	-0.6	-0.6	-0.4	-0.6	-0.6	-0.6	-0.6	-0.6
Soil Type E	0.0	-0.8	-1.2	-1.2	-1.0	-1.2	-0.8	-1.2	-0.8	-0.8	-0.4	-1.2	-0.4	-0.6	-0.8

FINAL SCORE, S

COMMENTS

Detailed Evaluation Required

YES   NO

* = Estimated, subjective, or unreliable data   BR = Braced frame   MRF = Moment-resisting frame   SW = Shear wall
DNK = Do Not Know   FD = Flexible diaphragm   RC = Reinforced concrete   TU = Tilt up
LM = Light metal   RD = Rigid diaphragm   URM INF = Unreinforced masonry infill

Fig. 2.4 Data collection forms by FEMA 154 (FEMA, 2002)

2.3.2   Hand-held equipment

Hand held equipment is used to collect field pictures and field notes referenced at the geographical coordinates of the location from where they were taken, all combined and incorporated into a Geographical Information System (GIS). Pictures can include additional information such as the distance to the object photographed and the direction of viewing.

Once structured into a GIS, the civil engineer is able to view the collected information and to tag the buildings with the appropriate attributes. This last step allows transforming the assembly of GIS data into an exposure database.

Some of these hand held equipment are now mounted on moving vehicles: i.e. cars, motorbikes or even bicycles. Their development was spurred by the need to rapidly collect damage information after a disaster. This has proven to be extremely effective, as it allows a few people with minimal time investment to collect large amounts of data that is then interpreted by specialists in the office.

Imaging with video and high through-put imaging cameras allows models of urban areas to be created that include the facades of all buildings. The technology at present is not mature enough to include full processing in an automatic way. However, the demand for such systems goes beyond crisis management applications. Before not too long entire streets will be imaged and reconstructed in 3D. Nevertheless, imaging the full extent of a city from the ground may not be justifiable for crisis management applications, owing to the following three reasons: 1) cost of acquiring field images, 2) inaccessibility of given parts of a city (i.e. informal settlements), and 3) cost of processing the imagery. At present, the combination of field pictures and remote sensing data may be considered as an acceptable compromise between the precision of the collected information and the extent of the area to be covered (Wieland et al 2012). A brief discussion of digital cameras, Geographical Position Systems (GPS) receivers and palmtops for collecting ground information is provided bellow.

2.3.3   Digital cameras

Pictures from digital cameras provide general information for image interpretation and risk assessment. Collecting the location of each image facilitates its integration with other spatially referenced information. The process of attaching location (e.g., latitude/longitude) information to pictures is also referred to as geo-tagging. Some digital cameras are equipped with GPS receivers that generate geo-tagged digital pictures. The most suitable equipment available in the market for fieldwork has a GPS receiver integrated in the camera with a positional accuracy of 1-5 meters. When the camera is switched on the GPS receiver searches for GPS signals, and when at least three satellites communicate with the GPS receiver the exact position is shown in the camera display. When the picture is taken, the GPS coordinates are saved within the image's Exchangeable Image File Format (Exif) file. Together with further metadata, such as date, time, focal length, shutter speed, and so on, the latitude and longitude (sometimes also altitude) coordinates are saved and can be later accessed using image processing or GIS tools.

Specialized software is available for processing field collected imagery and outputs to a full scale 3D building, inclusive of façade reconstruction. This software relies on a large collection of building pictures taken at different angles. Although the collection of images is not always possible and the reconstruction of the facade is time consuming, the output is of particular value since this allows for the geometric parameters of the typical European elements at risk to be interpreted.

2.3.4   GPS receivers

Positioning devices are used for locating the information collected in the field. GPS coordinates are linked to photographs using post-processing when pictures and location

information are collected independently. Location information needs to be collected with an external GPS device: by synchronizing the timestamps of coordinates and digital photos, every picture can be linked to a geographic position. When location information cannot be captured with the digital picture automatically, photos can still be geo-tagged by identifying the location of pictures from digital maps. For this method several software tools are available (e.g. Geosetter, which integrates Google Maps).

2.3.5 Palm tops

Personal Digital Assistants (PDAs) or Pocket PCs are often equipped with GPS receivers. In field work, a PDA is useful for data entry using forms that store information digitally and are readily linked to a GIS.

The JRC developed a tool which works on a Windows Phone (Windows FMC 6) that allows geo-localized data points to be collected, annotations and voice tagging to be added, distances and heights to be measured, and allows status images with buttons to be assigned (Annunziato 2010). The data collected in the field can be uploaded in real time to a server located in Ispra (Italy); then a website is available to download the data in several formats. The tool has been extensively used after the earthquakes in Haiti, Chile and in L'Aquila (Italy).

ROVER- Rapid Observation of Vulnerability and Estimation of Risk (McLane and Porter 2008) is a screening method based on the implementation of FEMA-154 on mobile smart phones (Fig. 2.5). It is essentially an automated walk-down method that allows for rapid assessment of the inventory of buildings and their vulnerabilities.

Fig. 2.5 A Windows Mobile Smartphone and a Bluetooth GPS device, and screen shots of the installed ROVER software for data collection

3 Integration of data sources for optimum inventory datasets

3.1 INTEGRATION OF DATA EXTRACTED FROM REMOTE SENSING IN A GIS ENVIRONMENT

Data integration involves the processing of different data layers in order to make them compatible with respect to spatial system (extent, projection system), data format and information content consistency. Once all the data are stored in a GIS database (geodatabase); they can be overlaid, queried, and analysed, obtaining statistical aggregation and spatial indicators that can be exploited in vulnerability analysis.

3.1.1 Built-up spatial metrics

Spatial metrics have been defined and applied in landscape patterns analysis to describe habitat configurations, functional connectivity and process-based relationships (O'Neil et al. 1988; McGarigaland Marks 1995; Alberti and Waddell 2000). In more general applications, these metrics can be used for spatially explicit analysis to assess the patterns of physical features, and to describe their geometry.

Spatial metrics have been used to characterize urban patterns in built-up and building stock analysis (Tenerelli and Ehrlich 2010, Xi et al. 2009).

Several spatial metrics can be applied for assessing the building exposure to risk, and can characterize the geometry and spatial pattern of buildings or building aggregates. These metrics can be grouped in three main categories: area/density, shape and proximity. The first two categories characterize single buildings or built-up units, while the last category of metrics can also characterizes the spatial relation between different built-up categories such as buildings and roads or open spaces. Area density indexes represent the number of buildings in the land unit. Shape indexes measure the building shape complexity. Proximity indexes measure the isolation of a building or the distance between each building and the nearest open space, road or critical infrastructure.

3.2 METHODS FOR COMBINING REMOTE SENSING, CENSUS AND FIELD DATA

Socio-economic data characterizes fundamental variables in vulnerability assessment; population data, in particular, are needed when performing estimates of casualties in natural disaster scenarios. The data are normally available from censuses, which account specific entities (i.e. people, household) as statistic aggregations at the level of arbitrary areal units. These units commonly correspond to administrative boundaries and do not have an intrinsic geographical meaning. Thematic maps which are based on such predefined areal units are also called cloropleth maps.

Socio-economic census data can be mapped using spatial disaggregation techniques (Eicher and Brewer 2001, Mrozinski and Cromley 1999, Chen 2002) which realistically place

non-spatially explicit attributes over geographical units (reporting zones). This is needed when performing analyses which integrate the census data with physical parameters (i.e. environmental data, built-up maps, topography) which follow natural boundaries or regular grid cells. The disaggregation techniques may be based on ancillary data which are normally related to the land use. These ancillary data can be extracted from remote sensing data.

In the following the methods that are used to map population density are described, focusing on the main downscaling techniques used in GIS modelling and the contribution of remote sensing in population density displacement models.

3.2.1 GIS modelling for population downscaling

The downscaling methods based on GIS can be classified as geostatistical methods and areal interpolation methods (Wu et al. 2006). In geostatistical models continuous density surfaces (isopleth maps) are produced using control points, which represent census values (Tobler 1979, Wu et al 2006, Wu et al. 2008). In addition to the population dataset, geostatistical models can be applied with or without ancillary information.

Areal interpolation methods are commonly used in population downscaling, they apply a homogeneous zone approach where the census units are disaggregated into smaller enumeration zones. Areal methods, which interpolate census data using ancillary information, are generally referred to as dasymetric, or "intelligent areal interpolations". Different techniques for dasymetric modelling exist. The dasymetric models normally apply one downscaling parameter. Dobson et al. (2000) applied a multi-dimensional dasymetric model which includes multiple physical parameters to map ambient population in 1km grid cells at the global scale (ORNL's LandScanTM). In dasymetric models, the categorical or continuous proxies are related to population through sampling techniques (Wu et al. 2008, Mennis 2003, Mennis and Hultgren 2006), regression analysis (Yuan et al. 1997, Wu et al. 2006, Chen 2002, Lu et al. 2010, Briggs et al. 2007) or expert knowledge (Eicher and Brewer 2001).

Another important distinction must be made between volume preserving methods and non-volume preserving methods. In volume preserving methods the pycnophylactic constraint is applied, which means that the sum of population from all zones coincide with the known population (Tobler, 1979, Gallego et al. 2011).

The criteria for the choice of method for population interpolation are the data availability and quality (accuracy, scale), together with the purpose of investigation. Dasymetric downscaling is particularly suitable for discrete variables with approximately homogeneous intra-zone distribution and inter-zones with actual changes, as is the case of many socioeconomic variables (Cai, 2006).

3.2.2 Contribution of remote sensing in population downscaling models

When disaggregating population distribution, remote sensing data can provide input proxies in three different approaches:

i. Extract the physical features that are then related to the population distribution. The most typically used features are the buildings and the built-up area. Physical feature classes can be extracted by manual digitalization and automatic or semiautomatic image classifications, based on spectral or textural parameters (Liu and Clarke 2002,

Yuan et al. 1997, Schneiderbauer and Ehrlich 2005, Holt et al. 2004, Dong et al. 2010, Lu et al. 2006).

ii. Extract textural or spectral parameters that are not classified in features classes, but are used as predictor variables in regression models at the pixel level (pixel-based approaches) (Azar et al. 2010, Li and Weng 2005, Lu et al. 2010, Lo 1995, Wu and Murray 2007).

iii. Combination of aerial interpolations at zones, blocks or land use class levels and regression models at the pixel or object level to obtain sub-zones population distributions (Chen 2002, Wu et al 2008, Wu et al 2006, Briggs et al. 2007, Harvey 2002).

4 Case Study: Vienna

4.1 DATABASE OF VIENNA CITY

The 20th district of Vienna (Fig. 4.1) is one of the SYNER-G test cases. The district consists of various types of buildings, with building practices that start from 1848 up until recently. In this area there are railroads/railway stations, underground and tramway lines, as well as bus lines and numerous very frequently used bridges across the Danube. There are numerous essential facilities like fire stations, police stations, schools, ambulance stations, an important hospital, the Millennium Tower (one of the tallest buildings in Vienna), etc. (SYNER-G 2010a).

All the information about the area, including buildings, transportation, bridges, etc., is gathered in various databases linked to a GIS. In the building database, every building is characterized by an identification number and the most essential details, including construction year, number of floors, existence of lofts/cellars and usage (Fig. 4.2). Additionally, the database has a photo-link to every building.

On the west and east side of the area there are many crucial bridges across the Danube. These bridges are the most important in terms of capacities for the city of Vienna. The bridge information is stored in a database, where the most important features are summarized, together with a picture. Fig. 4.3 shows an example of this database.

Fig. 4.1 Study area of Vienna city: the 20th district

number	floors	loft	cellar	construction year	construction era	construction era exact	usage	fotolink
371	4	n	y		1848-1918	1881-1890	res	yes
372	4	n	y		1848-1918	1881-1890	res	yes
373	4	n	y	1877	1848-1918	1881-1890	res	yes
375	5	n	y		1848-1918	1891-1900	res	yes
376	5	n	y		1848-1918	1881-1890	res	yes
377	3	n	n		-1848	1841-1850	res	yes
378	2	n	n		1848-1918	1871-1880	res	yes
379	5	n	y		1848-1918	1901-1910	res	yes
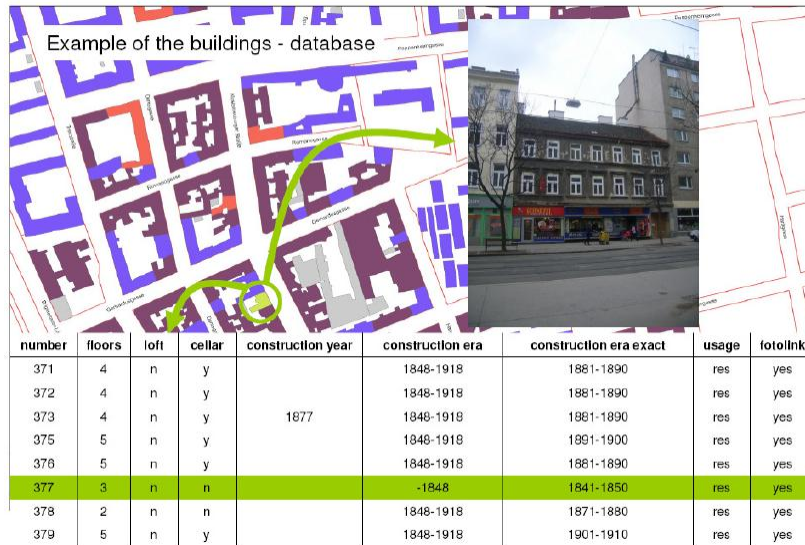
Fig. 4.2 Example of building database in Vienna
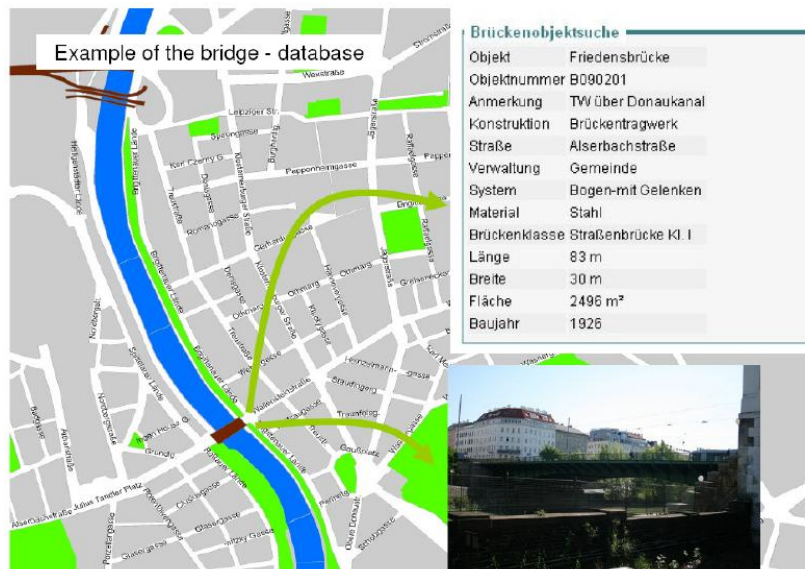
Fig. 4.3 Example of bridge database in Vienna

4.1.1   Building identification procedure (BIP)

The main purpose of this procedure is to identify and categorize buildings in a relatively big area (SYNER-G 2010b). The output of this procedure is a fact sheet for every building which contains all the information required to quantify earthquake vulnerability, and the overall condition of the building. The Data Collection Form includes space for documenting building identification information, including its use and size, a photograph of the building, and documentation of pertinent data related to seismic performance (Fig. 4.4). Buildings may be reviewed from the sidewalk without the benefit of building entry, structural drawings, or structural calculations. Reliability and confidence in building attribute determination are increased, however, if the structural framing system can be verified during interior inspection, or on the basis of a review of construction documents.

The BIP is completed for each building screened through execution of the following steps:

- o verifying and updating the building identification information;
- o walking around the building to identify its size and shape and looking for signs that identify the construction year;
- o determining and documenting the occupancy;
- o determining the construction type;
- o identifying the number of persons living/working in the building;
- o characterizing the building through the ground plan and determining the distance to traffic area;
- o characterizing the building elevation, using the laser telemeter to define building height;
- o identifying soft stories or added attic space;
- o identifying façade elements including the number of windows and doors;
- o determining non-structural members;
- o determining the overall condition of the building;
- o noting any irregularities/anomalies;
- o taking pictures with the digital camera.

Protocol for building identification procedure	Name.: Vukovic		
	Date: 29.04.2010	No.	23
	Time: 12:35		

Address:	Street / No.	Greiseneckergasse		3	
	PLZ	1200			
Photonumber:	from:	3626	to:	3641	01
Building Usage:		Club House/Residential (10/90)			02
GPS-Coordinates:					
Construction Year:					03

Construction Type	Masonry	X	04
	Reinforced Concrete		
	Steel Frame		
	Other:		

Persons/Dwelling Units	Number of Dwelling Units	18	05
	Number of Persons Working	2	06

Ground Plan	Corner Building			07
	Adjacent Buildings	right	X	08
		left	X	09
	Rectangular Ground Plan			10
	Distance to Traffic Area		5 m	11

Elevation	Number of Floors (inclusive Ground Floor)	7	12
	Building Height	17 m	13
	Shops at the Ground Floor	1	14
	Attic Space added	X	15
	Soft Story		14

Facade	Number of Windows and Doors		45	16
	Facade Design	none	X	17
		simple		
		detailed		
		very detailed		

Non-Structural Members		none	< 3	3	> 6	
	Chimneys		X			18
	Detailed Facade Elements	X		X		19
	Sculptures/Statues	X				20

Condition		none	few	many
21	Cracks	X		
22	Humidity/Efflorescence	X		
23	Damage on the Roof	X		

Anomalies Irregularities	24	Big Oriel from the first floor up

Fig. 4.4 Data collection form for buildings in Vienna city

4.2 REMOTE SENSING DATA

A vulnerability analysis of the building stock was tested for the case study of Vienna using satellite optical and radar data.

A radar image was available from the COSMO-SkyMed satellite on the Vienna study area, the main data parameters are presented in Table 4.1. Fig. 4.5 shows the radar image on the study area.

The optical data were available for Google Earth.

Table 4.1 SAR Data Features

Sensor Name	Acquisition Date	Acquisition Time	Acquisition Mode	Incidence Angle	Orbit
CSK-S1	01-Apr-2008	05:12	Enhanced Spotlight	49.13°	Ascending

Fig. 4.5 Radar data of the Vienna study area

4.2.1 Building and road parameters extraction

Starting from the radar and optical satellite image, the building footprints were manually extracted. A vector file was thus obtained (Fig. 4.6).

In order to estimate the number of storeys for each building, different information was exploited, such as shadows (both from optical and radar data), strong reflectors and also street view pictures of the structures provided by free tools such as Google Street View and Bing Maps.

In order to extract the main roads of the study area, a linear extractor, i.e. the W-Filter linear extractor (Negri et al, 2006), was used, as described in Dell'Acqua et al. (2011). The results are shown in Fig. 4.7.

Fig. 4.6 Shape file layer of the building stock in the study area of Vienna

Fig. 4.7 Road network extraction in Vienna

4.2.2 Building vulnerability assessment

Vulnerability assessment of a building can be performed given the footprint dimensions and number of storeys. This information can feed a model such as SP-BELA (Borzi et al., 2008a; Borzi et al., 2008b) to conduct a vulnerability study of a single building, and then a

vulnerability mapping for the entire building stock which is classified on the basis of pre-defined typologies.

Fig. 4.8 shows an example of extracting the number of storeys from radar imagery. Fig. 4.8-a shows that the most visible building façade is the North-Western one as it faces a wide urban road and it is not occluded by vegetation. The corresponding radar image (Fig. 4.8-b) features quite apparent rows of scatters, probably originated by the corner structures constituted by the protruding balconies, in addition to the corner reflector structure at the pavement/façade meeting point. If we assume that the footprint of the building is available, so is also the dominant direction of the façade in the image. Directional filtering enables turning such rows of scatters into a more homogeneous, linear bright area, which can be easily detected by the linear feature extractor, as seen in Fig. 4.8-c. Quite apparent are here the three parallel lines which mark the associated three storeys. Counting the longest parallel lines extracted from the image results in determining the number of storeys in the building. Repeating the same procedure on the next most visible façade, i.e. the northern one, provides the same result and confirms the previously obtained one (Fig. 4.8-d).

a)

b)

c)

d)
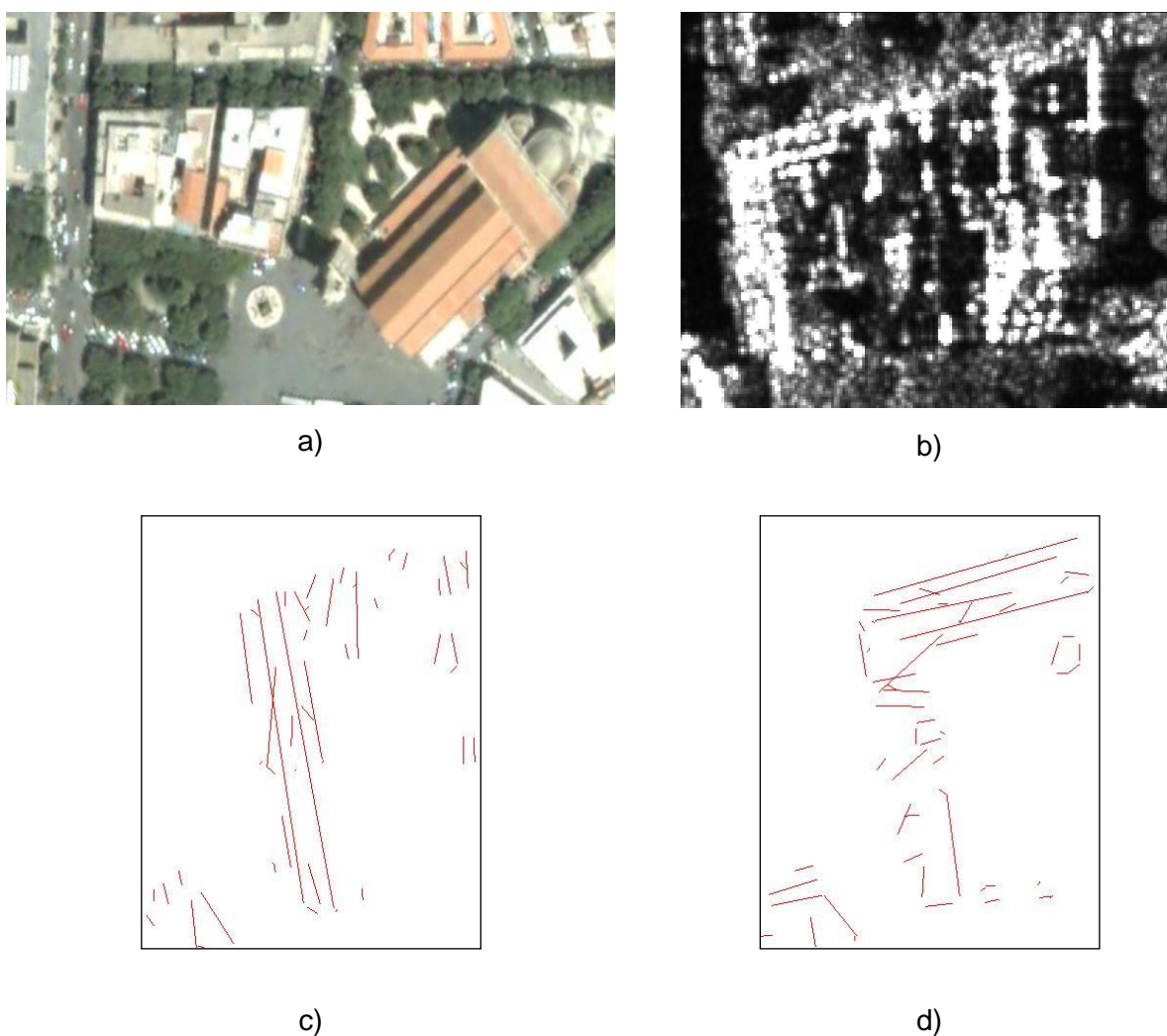
Fig. 4.8 a) The optical image from Google Earth; b) The SAR image of the selected building; c) Segments extracted from North-West façade; d) Segments extracted from North façade

Given the number of storeys and the footprint dimensions in both primary directions, SP-BELA calculates the probability that the building reaches or exceeds a certain damage state, e.g. slight, moderate, extensive and complete, for a given level of Peak Ground Acceleration (PGA).

Fig. 4.9 shows the results of a vulnerability analysis of a structure. The figure on the left shows the footprint of the building under study, it is a 4-storey building with footprint dimensions of 25 x 33 meters. On the right side the fragility curves for four damage states are plotted. The y-axis represents the probability that the building reaches or exceeds a certain damage state, e.g. slight (black line), moderate (blue line), extensive (red line) and complete (green line), for a given level of Peak Ground Acceleration (PGA).

The same analysis can be performed on the entire building stock, obtaining a vulnerability map for a given seismic hazard. An example of the possible results is shown in Fig. 4.10. This vulnerability map shows a possible output of a vulnerability analysis. It is possible to create different maps, changing the state limit of interest and the PGA value. Each building is classified according to the value of the structural fragility, represented on the map with a different colour.
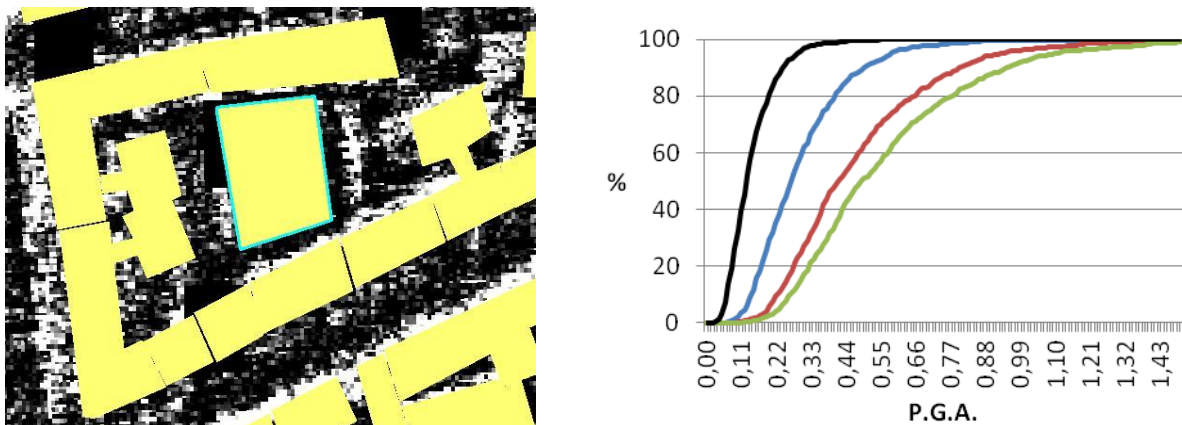
Fig. 4.9 Example of vulnerability study: the building under study marked by green rectangle (left) and its fragility curves (right)

Fig. 4.10 Example of building vulnerability mapping for the Vienna case study. Each colour corresponds to different levels of estimated vulnerabilities

4.3   COMBINING REMOTE SENSING AND POPULATION CENSUS DATA

A disaggregation model was applied to downscale the census population data for the city of Vienna using an urban land use map as ancillary data. The objective of this test was to downscale the population density derived from different census data at the level of building blocks.

The model applied for the Vienna case study is based on a dasymetric, or "intelligent areal interpolations" approach. Dasymetric models apply a homogeneous zone approach, where the census units are disaggregated into smaller enumeration areas, using ancillary information. Dasymetric mapping is commonly used for population downscaling when ancillary variables characterized by high correlation with population and high accuracy are available. The application of population interpolation based on ancillary data is becoming common with the increasing availability of land use/land cover data extracted from remote sensing and the progress in GIS technologies. The most typically used ancillary data is the land use map and the built-up physical element maps (buildings, roads, impervious area), which represent the living space of population. Gallego et al. (2011) described and compared different methods for assigning the ratio of population density to different land use classes, dividing them in two main classes: "fixed ratio methods", which assign the same ratio of density to all classes, and "limit-based methods", which apply upper limits to the population classes.

The methodology applied for the Vienna case study is a refined application of the one used by Gallego (2010) to produce the Population density grid of EU-27+ (version 5) (Fig. 2.2).

The ancillary data in this application is the Urban Atlas (UA) land use map (EEA, 2010), which covers the central city area and good part of the hinterland (Large Urban Zone), at a nominal scale of 1:10 000. Two different population census data were used as input for the downscaling (Fig. 4.11):

o a local population census on the central city area (about 290 km^2) - from 2001-available at the level of census polygon of approximately 25 ha in size;

o a country level population census - from 2006 - available at 1 km grid cells.

The study area was divided in a training area and a test area (Fig. 4.12). The training area was used for estimating the population density of each urban land use class (c) derived from the UA. The test area was used for testing and evaluating two different population downscaling method at 2 km resolution, the limiting variable and the fixed ratio method. The most accurate method was then applied to the all study area.

In order to take into account the different population density that occurs in the central city district and in the hinterland, the study area was also divided in two different zones: the central area zone (stratum 1) and the hinterland (stratum 2) (Fig. 4.12). The stratum 1 corresponds to the area where the local - polygon based - census is available. For the stratum 2 only the grid cell census was available.

The following paragraphs describe the modelling steps and the final result.
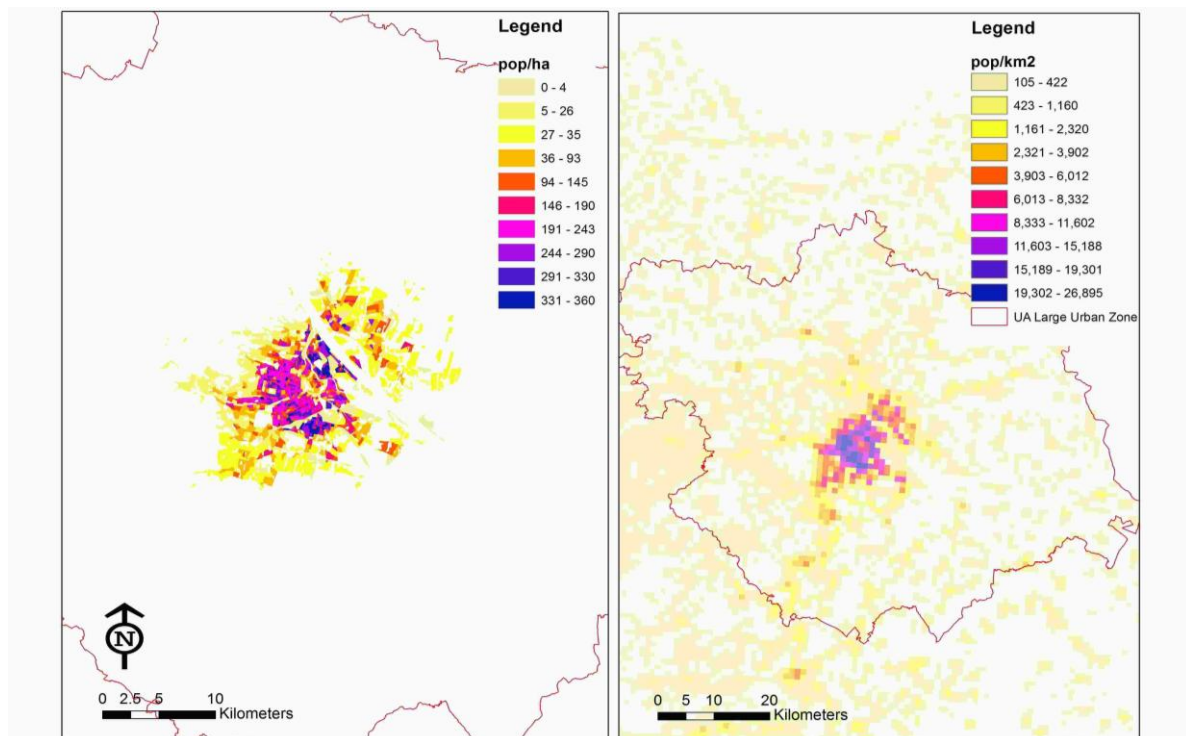
Fig. 4.11 Population census data for the Large Urban Zone of Vienna: local population census (left side), country level population census (right side)
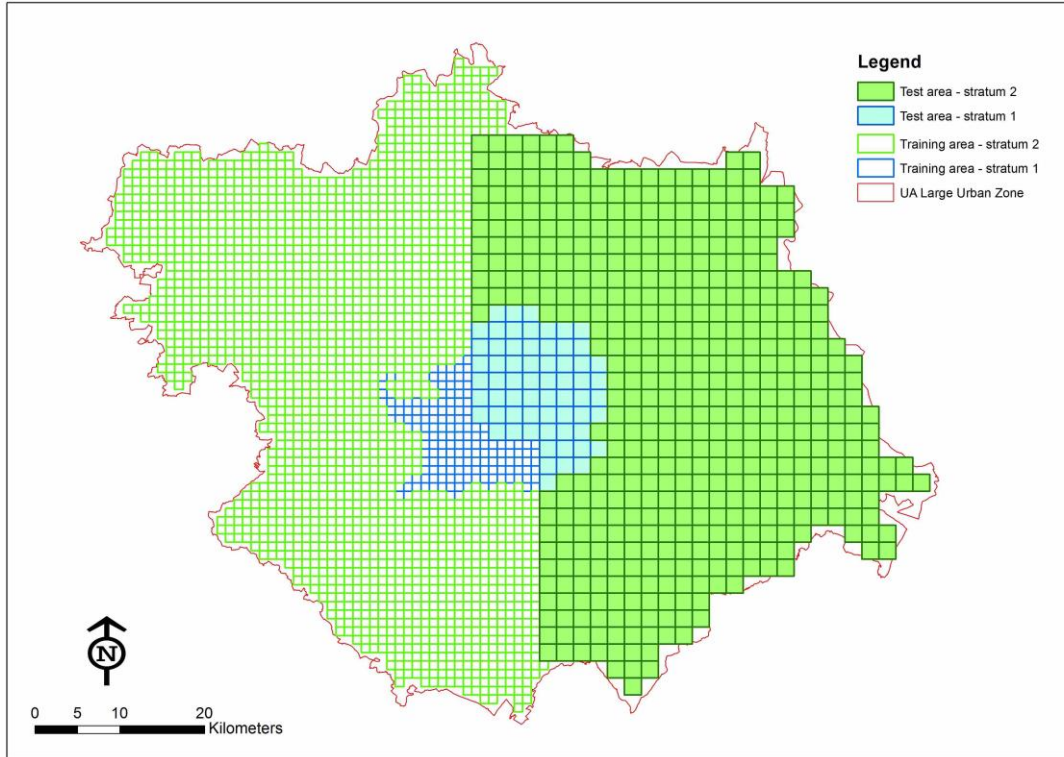
Fig. 4.12 Population zones for the study area in Vienna

4.3.1   Sampling of population density classes

The urban land use classes used to downscale the population density were derived from the UA classes through the class aggregation presented in Table 4.2. In order to assign the population density to each urban land use class, a set of sample polygons was selected in the training area. Those polygons correspond to census units which are covered by homogeneous urban land use classes (pure c census zone), excluding the "no population" land use area. The pure c census zone was selected according to the following condition (Eq. 4.1):

$$\frac{a_{cg}}{A_g - a_{no\ pop\ g}} > 0.80 \tag{5.1}$$

where:

a_{cg} = area of the urban land use class c in the census unit g;

A_g = total area of the census unit g;

$a_{no\ pop\ g}$ = total area of "no population" class in the census unit g.

In the hinterland area (stratum 2) the training samples (pure c census zone) correspond to grid cells, while in the central area the samples correspond to census polygons.

The population density of each urban land use class was calculated as the average population density of the class samples weighted by the area. The final population density for each class and each stratum are listed in Table 4.2.

Table 4.2 Population density values for each urban land use class and each stratum

UA classes	Urban land use class (c)	Cd_{s1}*	Cd_{s2}*	Ranking (*r*)
Continuous Urban Fabric	Continuous Urban Fabric	250.800	1.306	1
Discontinuous Dense Urban Fabric	Discontinuous Dense Urban Fabric	153.680	0.800	2
Discontinuous Medium Density Urban Fabric	Discontinuous Medium Density Urban Fabric	74.160	0.272	3
Discontinuous Low Density Urban Fabric	Discontinuous Low Density Urban Fabric	25.200	0.272	4
Discontinuous Very Low Density Urban Fabric; Isolated Structures	Discontinuous Very Low Density and Isolated Urban Fabric	0.859	0.004	6
Airports; Construction sites; Industrial, commercial, public, military and private units; Port areas; Sports and leisure facilities	Preliminarily Non Residential	17.560	0.040	5
Fast transit roads and associated land; Other roads and associated land; Railways and associated land; Agricultural and others**	No population	0.000	0.000	7

* Cd_{s1} = class density for the stratum 1; Cd_{s2} = class density for the stratum 2.

** Others = Semi-natural areas; Wetlands; Forests; Green urban areas; Land without current use; Mineral extraction and dump sites; Water bodies.

4.3.2   Fixed ratio method

In the test area the population count of each 2 km grid cell was disaggregated, per each stratum, at the level of the urban land use class units, according to the following Eq. (4.2):

$$P_{cg} = \frac{P_g \times Cd_{csx}}{\sum_c a_{cg} \times Cd_{csx}}$$

(5.2)

P_{cg} = population density of the urban land use class *c,* in the census unit (2 km grid cell) g;

P_g = total population in the census unit g;

Cd_{csx} = population density for the land use class *c*, in the stratum *sx*;

a_{cg} = area of the land use class c, in the census unit g.

4.3.3 Limiting variable method

The limiting variable method is described through the following steps (Gallego et al., 2011):

o   a uniform population density value derived from the original census dataset is assigned to all the land use polygons in each 2 km grid cell (D_g);

o   the land use classes are ranked and an index (r) is assigned from the lowest to the highest population density value (from "Continuous Urban Fabric"- r=1 – to "No population" - r=7) (Table 1);

o   If the D_g is above the population class density of the given stratum, the density value is modified: the population density become equal to Cd_{s1} or Cd_{s2} , and the population in excess is redistributed among the more dense classes according to the following Eq. (4.3) (Gallego et al., 2011):

$$P_{cg}^{r'} = D_g + \frac{a_{cg}^{r} \times \left(D_g - Cd_{csx} \right)}{\sum_{r''>r} a_{cg}^{r}} \tag{5.3}$$

this step is iterated for each $r' > r$: 7 iterations in total, one for each land use class, were performed;

o   at the end of the process if there is still some excess population it is redistributed to all the land use classes proportionally to the class density (Cd_{s1} or Cd_{s2}).

4.3.4 Selection and application of the model

The disaggregated population map resulting from the two tests were re-aggregated at 1 km grid and compared with the original 1 km census population grid. This was done for evaluating the two models, in absence of reference data.

The correlation analysis between the observed and the model-simulated data indicated a similar performance for the two models, showing a coefficient of determination (r2) of about 0.93 for both the model outputs (Table 4.3).

The agreement with the reference population grid was estimated, for each model output, in terms of Total Absolute Error (TAE), which is calculated as the sum of the residual absolute value. The TAE measures the average model-performance error in a way which is less ambiguous (Willmott and Matsuura 2005) and more robust in the presence of outliers (Gallego et al. 2011, Legates and McCabe 1999) than the commonly used Root Mean Square Error (RMSE). The TAE of the fixed ratio model was slightly lower than that of the limiting variable model (Table 4.3). The fixed ratio method was therefore applied to the whole study area (test area plus training area), for each 1km grid cell.

Table 4.3 Statistic indicators for each model output comparison with the reference population data

Statistic indicator	Limiting variable model	Fixed ratio model
r^2	0.931	0.936
TAE	260241	242334

4.3.5   Results

The map in Figure 4.13 shows the final disaggregated population map.

The tested methods preserve the pycnophylactic property which means that the original total population set (from the 1km grid census) is preserved. The advantage of this modelling is to have a population density disaggregated to spatial units which have homogeneous size and are usually smaller than the original census dataset. This spatial detail can affect the information accuracy on human exposure when the population map is used in risk assessment models.

The main limitation of this method is the difficulty of getting a population reference dataset suitable to obtain a sufficient sample of census unit covered by single land use class. Most of the census datasets, in fact, have a too coarse spatial unit. In this case study the two population census dataset were enough detailed to allow the collection of an appropriate sample number both in the central city area and in the peri-urban area.

This application only deals with residential population; it is therefore suitable for casualty estimations in night-time scenarios. Time-specific population maps are much more useful for human exposure analysis in disaster risk assessment. The data that are necessary to perform population spatio-temporal analysis (mobile population database and activity location map) were not available at the local level for the SYNER-G case studies. However the building vulnerability analysis in the SYNER-G project deals mainly with residential building typologies, therefore the disaggregated population map can be used together with the available building fragility data to perform a population vulnerability analysis for night time scenarios.
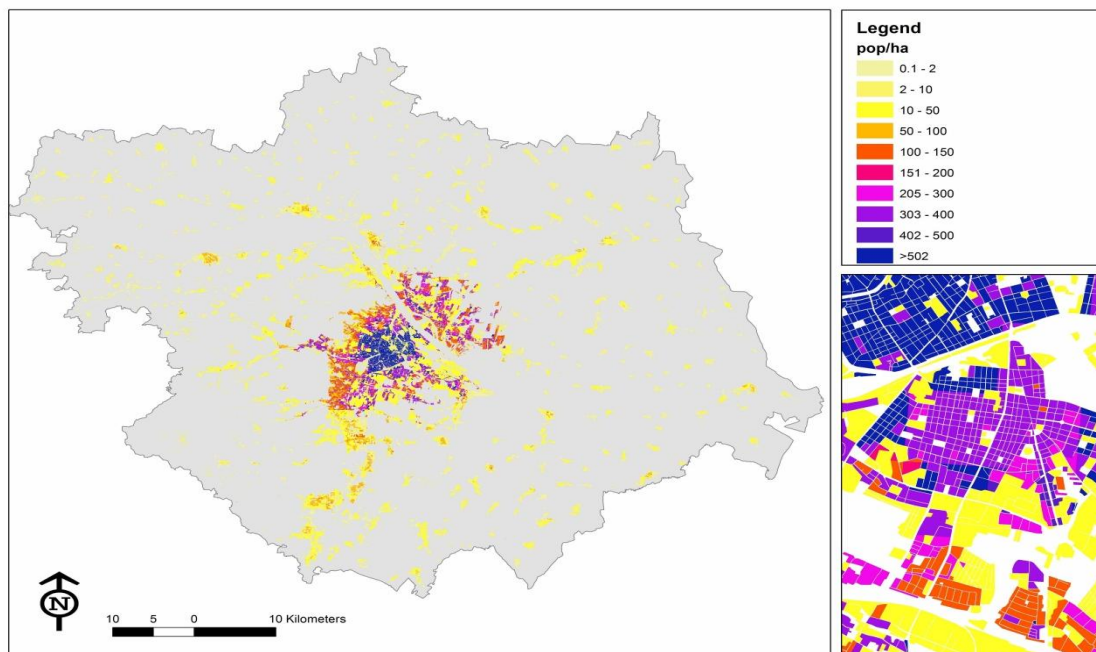
Fig. 4.13 Disaggregated population density map for the Vienna Large Urban Zone

5 Case Study: Thessaloniki

5.1 DATABASE OF THESSALONIKI CITY

The database of Thessaloniki city includes components of roadway, railway, port, potable water, wastewater, gas, electric power, telecommunication, fire-fighting and health-care systems, as well as buildings. The database was implemented between 2003 and 2006, in the Greek Geodetic Reference System (EGSA'87). In some areas data are missing, mainly due to the fact that networks are old (e.g. sometimes the material or location of water pipes is unknown), or the lack of organized data of lifeline owners/managers, especially for old constructions (e.g. bridges). The data of Thessaloniki inventory were collected based on the following methods:

- o census (ordinary buildings, population data, land use);
- o ground surveys (bridges, lifeline and strategic buildings, hospital buildings, port facilities);
- o GIS digitization of conventional maps (waste water network) or implementation studies (gas network);
- o existing databases from lifeline companies (water system, railway network, telecommunication network);
- o collection of data from authorities/companies' conventional archives (bridges, port facilities, electric power, railway elements, hospital facilities);
- o interviews with engineers of authorities or other lifeline companies (hospital facilities, port facilities, railway, electric power and telecommunication components);
- o LIDAR technique (road lines, building blocks and building footprints);
- o estimations and expert judgement (urban information);
- o the combination of all of the above.

5.1.1 Buildings

The current detailed building inventory covers about 40% of the municipality of Thessaloniki and refers to half of the blocks within this area (Fig. 5.1). This inventory is based on a combination of the 1991 census data, from the Statistics Agency of Greece, with data collected in a previous project (Penelis et al. 1988) through an in situ survey for 5047 buildings in 470 blocks (75% of which were situated in the municipality of Thessaloniki), following the 1978 earthquake. A "block-by-block" analysis was carried out in a selected part of the city where most of the damage from the 1978 earthquake occurred, using a new in-situ collection of data for 50 blocks. This in-situ work covered a selected sample (more than 10%) of the 470 blocks covered by the survey carried out in 1984-86.

The current inventory contains 5047 buildings out of 19 000 buildings in the municipality. The composition of buildings (including all the categories of the pre-defined Building Typology

Matrix - BTM) for the entire municipality can be estimated assuming that the composition of the surveyed area is representative of that of the entire municipality (Kappos et al. 2008).
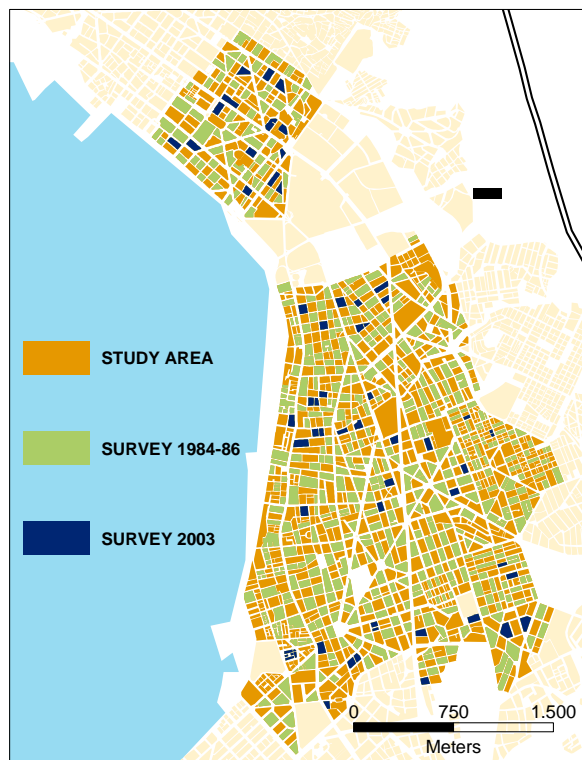
Fig. 5.1 Study area of Thessaloniki including the "block-by-block" analyses of 1984-86 and 2003

5.1.2   Roadway bridges

The database covers the metropolitan area of Thessaloniki, including 80 bridges constructed up until 2005 (Fig. 5.2). The data were collected from the public work authorities, private civil engineering companies and in situ surveys (Argyroudis et al. 2010). The inventory (Fig. 5.3) includes general information (e.g. location, year of design), geometrical (e.g. number of spans, length, skewness), technical (e.g. type of superstructure, bearings, piers, abutments, foundation) and geotechnical (soil type) parameters, and photographical data. In cases where it was not possible to obtain suitable data, appropriate estimations were made. For example, instead of the exact year of design, the period of construction was inferred from the known age of adjacent civil works in the same road axis, or from the experience of engineers from the transportation authority. During the SYNER-G project the database has been updated, where possible, to include further information (e.g. dimensions of bearings, reinforcement details of columns) for the development of numerical fragility curves. In addition, the start and end nodes of each bridge have been defined for the seismic risk analysis of the overall roadway system.
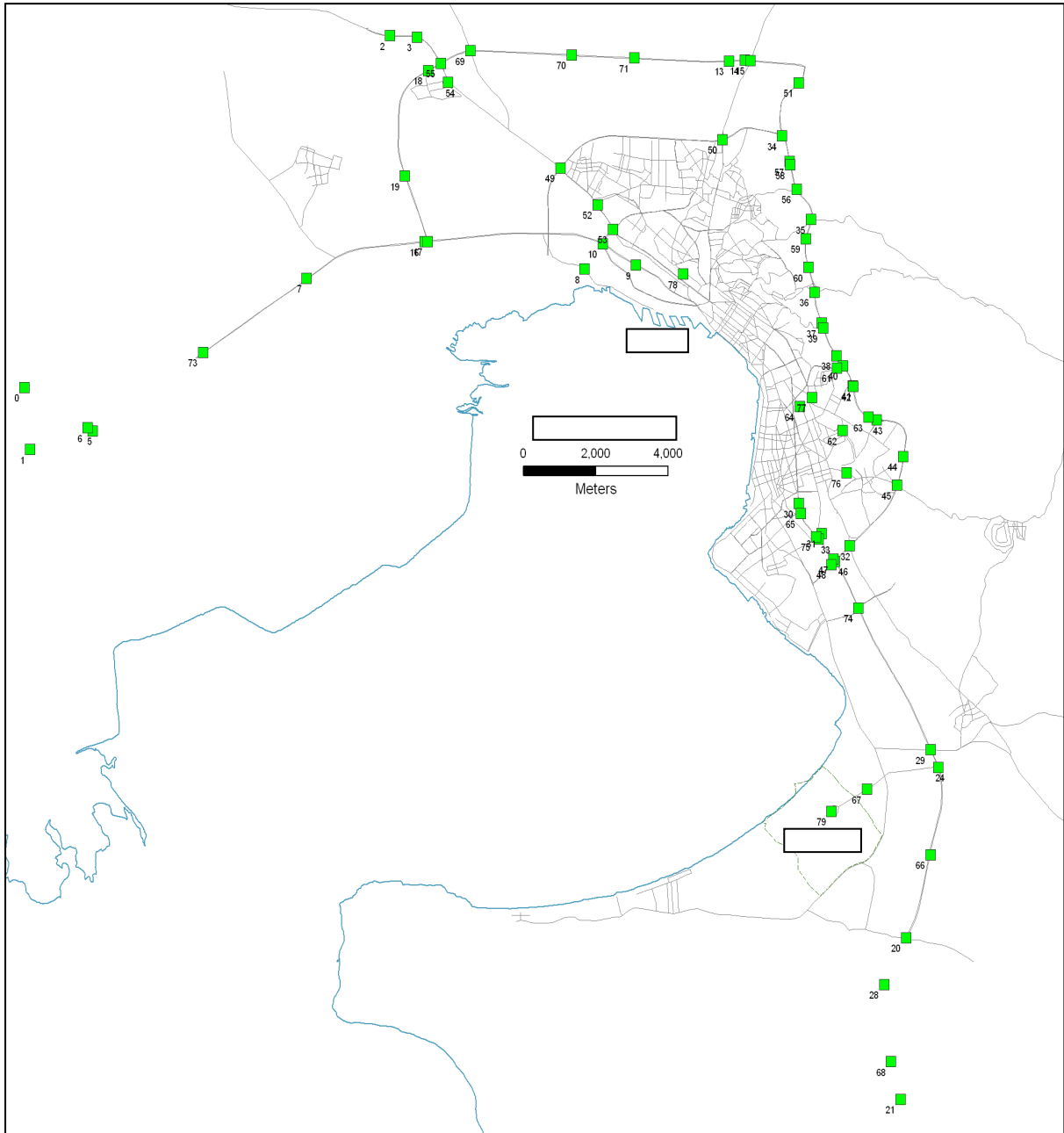
Fig. 5.2 Roadway bridges of Thessaloniki

INVENTORY SHEET FOR ROADWAY BRIDGE							
Date:			**Bridge ID:**				
GENERAL INFORMATION							
Name/Location of bridge:							
Year of construction:							
Contractor - Designer:							
GEOMETRICAL CHARACTERISTICS							
Number of spans:							
Length of spans (m):							
Total length (m):			**Width (m):**				
Different pier heights:	**Regular**		**Irregular**				
Alignment of bridge:	**Skewed**		**Straight**				
Skewness (^{0}):							
Comments:							
TECHNICAL CHARACTERISTICS							
SUPERSTRUCTURE							
Type-Material:							
Pier-Deck connection:							
Continuous superstructure:	**Yes**		**No**				
Number of intermediate joints:							
Comments:							
BEARINGS							
Bearings type:							
Support length:							
Comments:							
PIERS							
Pier type:	**Single column**		**Multi column**		**Wall**		
Maximum height (m):							
Foundation type:							
Comments:							
ABUTMENTS							
Abutment type:							
Foundation type:							
Comments:							
SOIL							
Description:							
Soil class:							

Fig. 5.3 Inventory sheet used for the collection of data for roadway bridges in Thessaloniki

5.2   REMOTE SENSING DATA

Different information mining techniques were tested for the case study of Thessaloniki, focusing on the exploitation of Very High Resolution (VHR) optical remote sensing. The tests were conducted for the extraction of building parameters.

A GeoEye-1 image which covers about 16.5 km^2 was available for the analysis. The image was collected in March 2010 with a resolution of 0.5 meter for the panchromatic band (black & white) and 2 meter for the multispectral bands (blue, green, red, near IR). Fig. 5.4 shows the true colour band composition of the ortho-rectified and pan-sharpened image.

The following sections summarize the tests which were performed for extracting the building count, built-up area and building height.
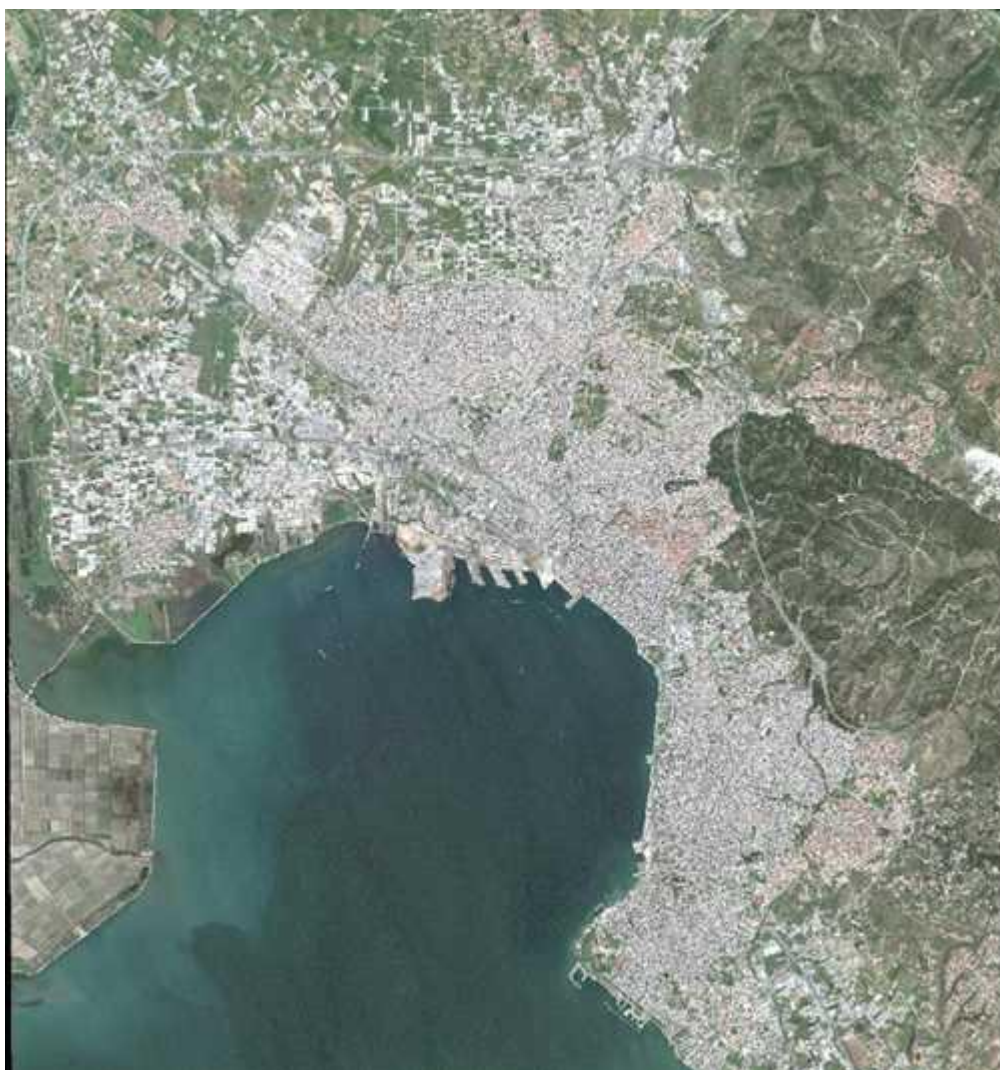
Fig. 5.4 VHR multispectral image of Thessaloniki city and its hinterland from GeoEye. The panchromatic band was used to enhance the spatial resolution of the multi-spectral bands using the Gran Smith pan-sharpening technique.

5.2.1 Building count

The existing building inventory for Thessaloniki city provides a footprint location map. This footprint map can be used to estimate the number of buildings within each block of the study area (central city district). However, in some blocks this information is missing, or needs to be updated, and/or there is a critical geometric mismatch between the mapped building footprints and the actual building position on the satellite image, especially over the hilly areas of the city.

In order to have a complete and consistent estimation of the number of buildings per block, the existing dataset was updated with a visual photo-interpretation of the pan-sharpened GeoEye image, for 680 blocks. A point label was created per each building location, at the footprint centroid.

If photo-interpretation is used to detect the number of buildings, the criteria for the identification of each single building need to be clearly defined. The criteria are generally based on the elements which can be distinguished from the satellite image at the given observation scale. For this case study the following criteria were considered to define and distinguish each building unit:

- o   visible difference in the roof colour;
- o   visible distance from the next building;
- o   visible difference in the building height.

Fig. 5.5 shows two satellite image snapshots on the central area of the city. The figure shows that the criteria used to distinguish each separate building are applicable at the given resolution, however, in some cases (see right image) there may be uncertainties in the interpretation of the image due to the very high building density, or to the presence of features on the building roofs that are not clearly distinguishable. Moreover, when performing a photo-interpretation of the building location or building footprints, the definition of one single building may differ from the definition which is applied when the inventory is performed from the ground. In fact many more structural and functional elements can be distinguished from ground surveys of buildings. These limitations should be taken into account when using remote sensing data to derive the building stock for vulnerability assessment.

Fig. 5.6 shows the building count map, which displays the estimated building number per block in the study area.

The building count represents a critical parameter when performing vulnerability analysis, in fact it can be used to stratify the building typologies when the typology information is available as statistical aggregation at the level of administrative zone or building blocks. The photo interpretation of the building count from VHR remote sensing data represents a very valuable data source when no ground survey is available, or for updating partially available datasets.
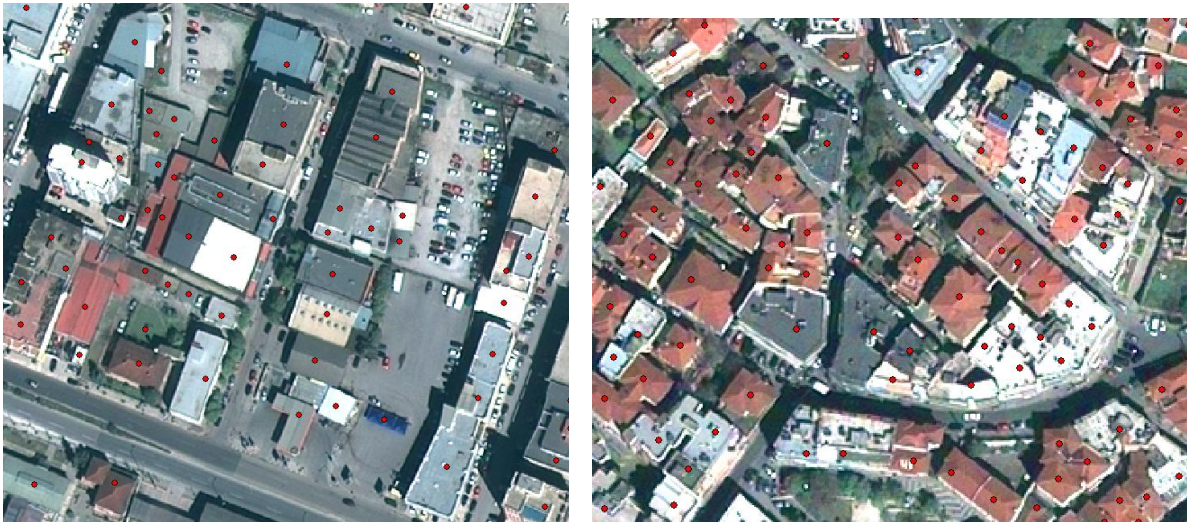
Fig. 5.5 Snapshots from the GeoEye image on the central area of the city. The red spots represent the photo-interpreted building centroids
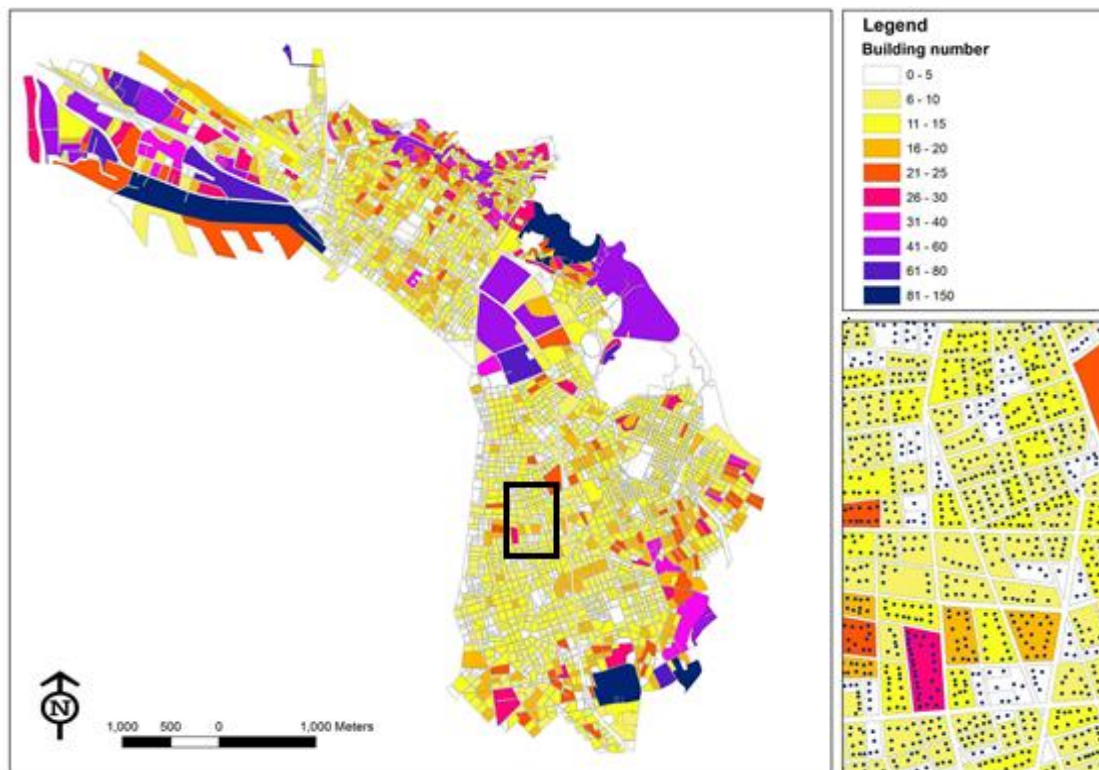
Fig. 5.6 Building count map showing the estimated number of buildings in the study area of Thessaloniki

5.2.2   Building area extraction

An automatic building area extraction was tested using the GeoEye image on Thessaloniki. The applied algorithm is based on the combination of the Differential Morphological Profile (DMP) and the PANTEX built-up presence index (Pesaresi et al. 2012). The DMP is a multi-scale image processing algorithm which can be used for automated extraction of urban features. This algorithm performs an image decomposition based on the morphological

characteristic of connected components (Persaresi and Benediktsson 2001). The applied model represents the DMP vector fields in three characteristic parameters, Characteristic scale, Saliency and Level (CSL model) (Pesaresi et al. 2012), and fuses it with the PANTEX built-up presence index. The PANTEX index (Pesaresi et al. 2008) exploits the high textural contrast available on built-up area and provides high values of digital numbers for highly contrasted urban areas and low values for homogeneous zones typical of non-built-up areas. This index shows the presence of buildings including surrounding physical elements such as roads, infrastructures, parking lots and remaining open spaces. For this case study, the index was calculated over a window of 50x50 m and the final built-up index was generalized at 2x2 m pixel size.

Table 5.1 Building area confusion matrix parameters

Overall Accuracy (%)	70.30	
Kappa Coefficient	0.34	
Confidence level (%)	95	
	Accuracy (%)	
Class	Producer	User
Non built-up	76.22	78.95
Built-up	58.11	54.25
Total	67.16	66.60
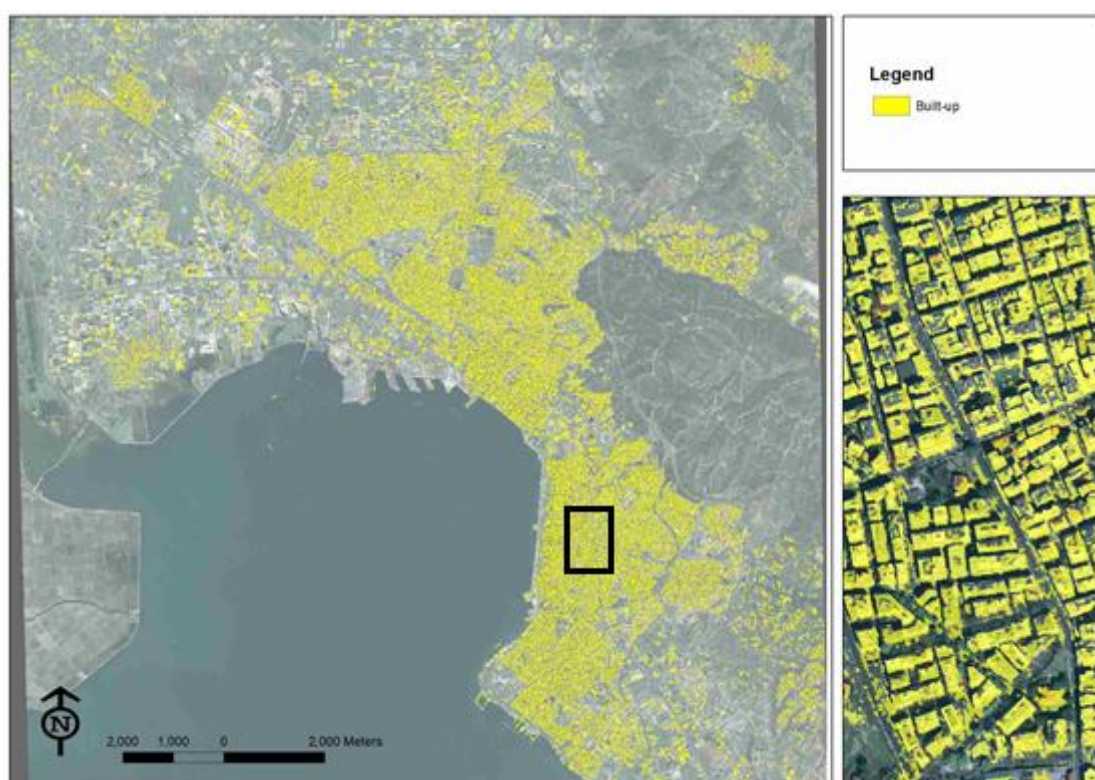
Fig. 5.7 Map showing the identified built-up areas in Thessaloniki

Fig. 5.7 shows the estimated built-up area. The final built-up index was compared with the reference building footprint map for the blocks where the footprints were available (1692 blocks in total). To assess the accuracy of the procedure, the built-up area derived from the built-up index was compared with that of the reference building footprint at 1 m resolution. A confusion matrix was thus calculated. The overall accuracy is of 70.3%. The map disagreement is mainly explained by the different scales at which the reference building footprint map and the automatically extracted built-up map were produced.

5.2.3 Building height extraction

An automatic building height extraction from the GeoEye image was tested by the length of the shadow casted by buildings. This approach has already been applied by several authors (e.g. Miura et al. 2004, Miura and Midorikawa 2006, Noronha and Nevatia 2001, Shao et al. 2011, Brunner et al. 2010). The technique is based on the following parameters: i) length of the shadow, ii) satellite viewing angle, iii) sun elevation at the acquisition time. The method is therefore suitable for images with specific acquisition parameters; its performance is also related to the building density and the building height. The ideal scenario is determined by the following conditions (Soille and Pesaresi 2011):

o image acquisition with view angle close to the nadir, so that building facades are not visible;

o sun elevation angle not too high: optimal value depends on building height, the acceptable maximum sun elevation angle increases with the building height;

o isolated building, so that casted shadows are fully visible.

The applied algorithm produced a height index which was generalized at 50m resolution. The height index values were then extracted on the given set of points representing the building centroids (building location map). The value of the building height was calculated from the adjacent cells using bilinear interpolation. The building height values were recorded in the attribute table of the building location map.

The building height values were then classified on the basis of the storey numbers. For this purpose an average storey height of 4 meters for the ground floor, and 3 meters for the upper floors, was considered.

The values of the building storey numbers were finally generalized to a larger spatial unit in order to take into account the approximation level of this methodology and to allow the comparison with the reference data. The considered spatial unit is the building block as defined in the available building inventory.

Fig. 5.8 shows the final map of average building storeys aggregated at the building block level.

The estimated values of average storey number per block were compared with the reference data available from the building inventory. The comparison was performed for the blocks with an area greater than 2500 m^2 - 1692 blocks in total - corresponding to the spatial resolution of the estimated height values (50 m). The correlation between the estimated storey number and the reference value was of 0.37 (Table 5.2).

The low correlation is due to the sensor parameter limitation. The GeoEye image used for this test was, in fact, acquired from a catalogue with standard acquisition parameters which are not optimal for obtaining a precise extraction of the building heights. The best results

were found for isolated buildings, where casted shadows are fully visible, however in the area of interest where the test was performed most of the surface is covered by very high building density.

The most suitable remote sensing technique to derive building height is represented by very high resolution stereo imagery, which is now available also from satellite platforms. Those data often allow a precise detection of the building height, depending on the resolution of the input imagery, the imaging angles and the type of processing. For the SYNER-G case study no stereo imagery was available.

Table 5.2 Regression statistics on the estimated number of storeys

Parameter	value
Observations (blocks)	1692
Multiple R	0.6044
R Square	0.3653
RMSE	1.6717
F	973
p-value	4.4719E-169
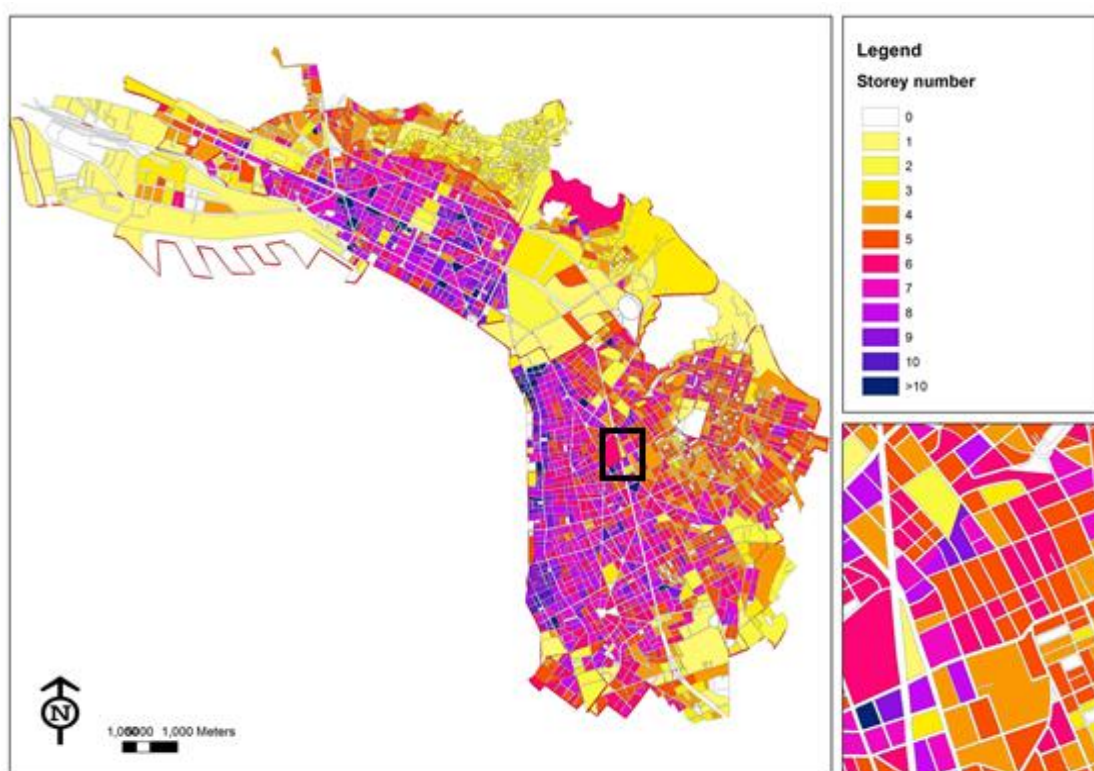
Fig. 5.8 Map showing the estimated number of storeys in the study area of Thessaloniki

5.3   GEOMETRIC ATTRIBUTES AND SPATIAL METRICS

Geographic layers can be analysed in GIS environment in order to get geometric attributes and spatial associations. For the case study of Thessaloniki some spatial metrics were applied to the vector layers of building footprints and transportation network. To perform the analysis all the data were integrated and stored in a geo-database.

Two different spatial metrics were applied to assess the spatial relation and geometric attributes of the building footprints and transportation network layers: the Shape index and the NEAR index (McGarigal and Marks, 1995). The building footprint and main road layer were derived from the existing inventory, while the transportation network layer was derived from the Urban Atlas (EEA, 2010).

The Shape index (SHAPE) was applied as a measure of the building shape complexity, according to the following Eq. (5.1):

$$SHAPE = \frac{p_i}{min_{p_i}}$$
(6.1)

where:

p_i total perimeter of building *i* (given the number of cell surfaces);

min_{pi} minimum perimeter possible for a maximally compact building (in a square raster format) of the corresponding building area.

The *SHAPE* index equals 1 when the building is maximally compact and increases without limit as the shape becomes more irregular. Fig. 5.9 shows the building SHAPE index map for a subset of the Thessaloniki study area. This result shows that when the SHAPE index value is higher than 1.5 there is a very high probability to have a complex building footprint shape, such as "T" shape, "L" shape, or very elongated rectangular buildings. Those buildings are commonly more vulnerable than buildings characterized by a squared, compact shape.

The NEAR index measures the Euclidean distance between each building and the nearest feature. The distance is measured in meters from the boundary edges. The NEAR index was applied for the case study of Thessaloniki to perform the following proximity analysis:

o   from each building to the nearest building;

o   from each building to the nearest main road;

o   from each building to the nearest transportation network feature - including fast transit roads, secondary roads, railways and associated lands (enclosed areas, parking lots, embankments, fenced areas along roads, railway facilities).

When applied to measure the building to building distance the NEAR index increases as the neighbourhood is increasingly occupied by other buildings and as those buildings become closer and more contiguously distributed. This index can be used to measure the isolation of a building or the distance to the nearest building characterized by a given typology. When applied to the building to road or transportation network, the NEAR index measures the distance between each building and the nearest road or railway or associated land. Fig. 5.10 shows the map of the Building to Building NEAR index. Fig. 5.11 and 5.12 show the maps of the NEAR index applied, respectively, to Building to Main Road system, and to Building to Road Network system.
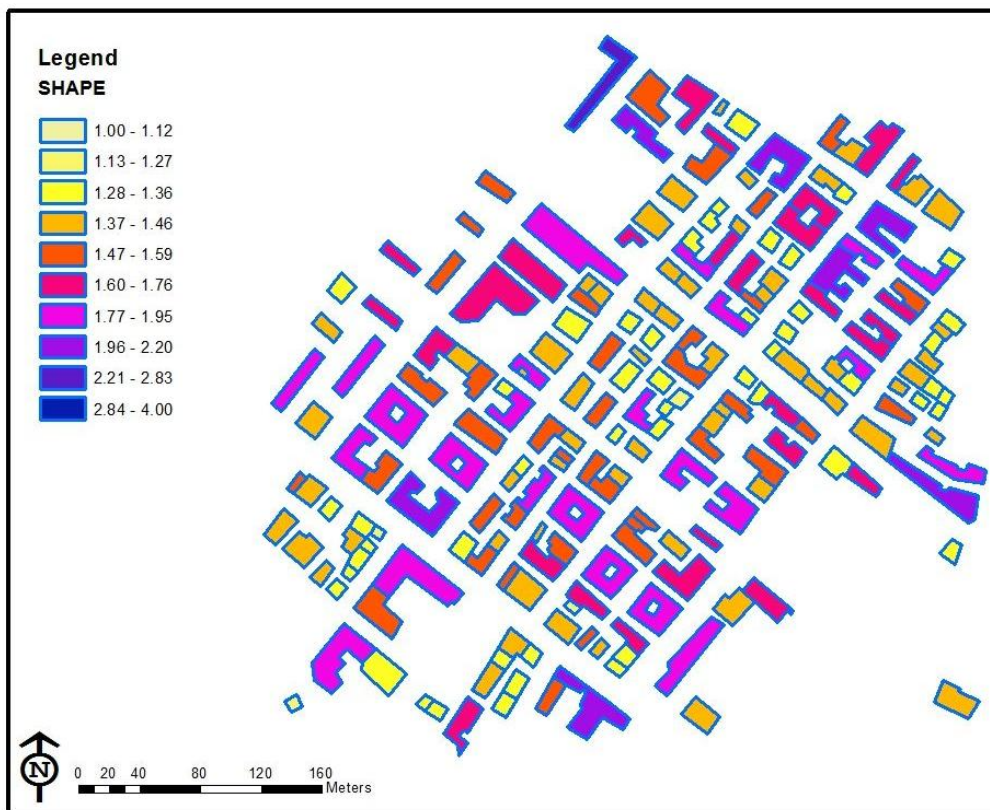
Fig. 5.9 Map showing the Building SHAPE index in the study area of Thessaloniki

Fig. 5.10 Map showing the NEAR index for Building to Building proximity analysis in the study area of Thessaloniki
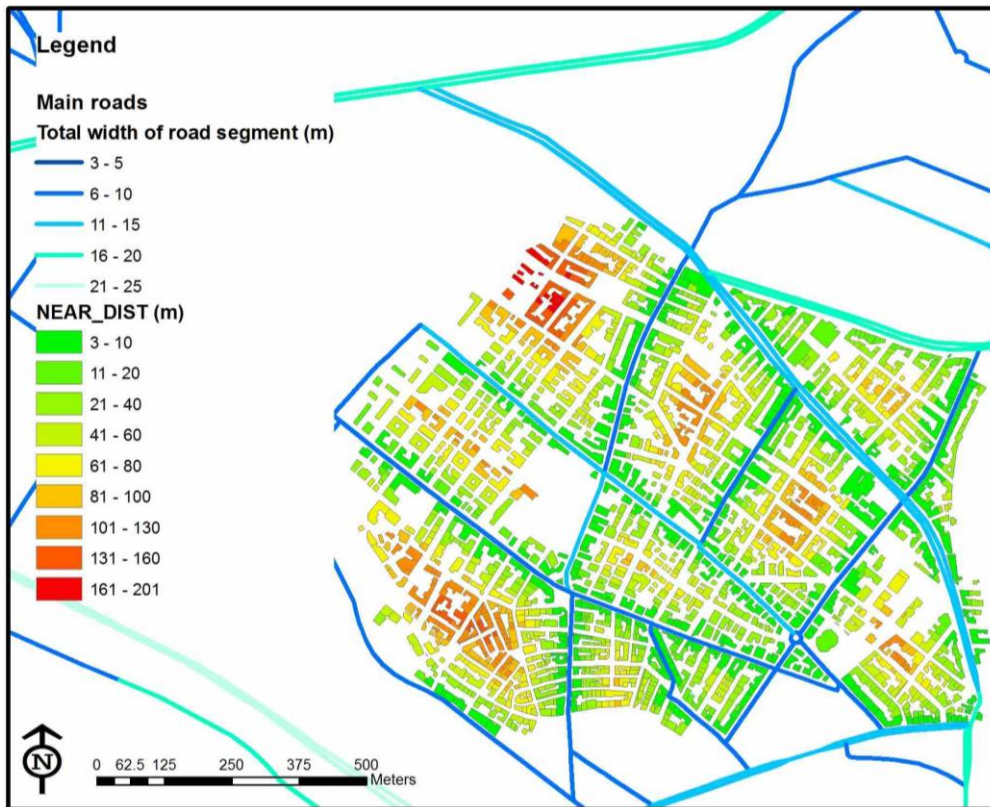
Fig. 5.11 Map showing the NEAR index for Building to Main Road proximity analysis in the study area of Thessaloniki
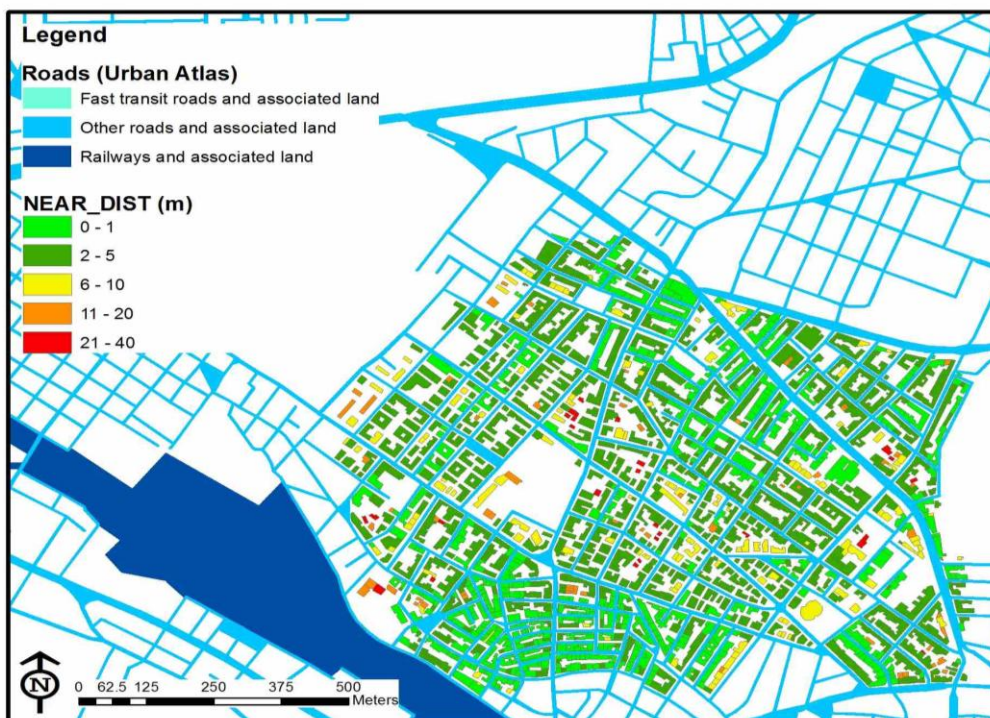
Fig. 5.12 Map showing NEAR index for Building to Transportation Network proximity analysis in the study area of Thessalonik

49

Spatial metrics, such as the SHAPE and the NEAR indexes, can be stored as attributes in a vector file and then used in risk assessment applications or emergency evacuation plans. For example the NEAR index can be applied to evaluate the road closure risk due to the collapse of a near building of a given typology. This index can also be applied to assess the distance of a given point or building to the nearest utility network (electric power system, gas and oil network, water system), or critical infrastructure (healthcare facilities, fire fighting system).

6   Case Study: Messina

The analysis was performed on a small area situated in the city of Messina, Italy.

A COSMO-SkyMed image was available (see Table 6.1) and free optical data was used (Google Earth and Bing Maps).

Table 6.1 Data Features

Sensor Name	Acquisition Date	Acquisition Time	Acquisition Mode	Incidence Angle	Orbit
CSK-S1	23-APR-08	05:21	ENHANCED SPOTLIGHT	50.57°	ASCENDING

Fig. 6.1 Optical (left) and radar (right) data of the case study area

In Fig. 6.1 an optical image with a polygon of the area of interest (left) and the radar data of the same area (right) are shown with a vector file representing the footprints of the buildings under study. Several researchers have developed image analysis and segmentation techniques to automatically extract urban regions and patterns from VHR optical data (i.e. Taubenböck et al. 2011, Gamba et al. 2009, Gueguen et al. 2011-a, Ouzounis and Soille 2010). In this analysis building footprint extraction is based on the aggregation of pixels with homogeneous spectral or spatial parameters (i.e. texture, scale, shape, size, brightness). This is done by computing these parameters from the original image and then classifying them along the original image with a supervised classificator; this latter step uses a routine able to modify, discard and reshape each primitive classified blob (group of interconnected pixel) in a final rectangular shape on the basis of thresholds selected by the user. The results of a recently advanced multi-scale decomposition scheme (Ouzounis et al. 2011) is the partitioning of the input domain into explicit layers of the image content based on

structural and shape attributes. These layers represent consistent sets of targeted patterns that can be further classified following different approaches to meet the final objective.

The number of storeys was extracted using the same methods of the Vienna case study, exploiting shadows and strong scatters.
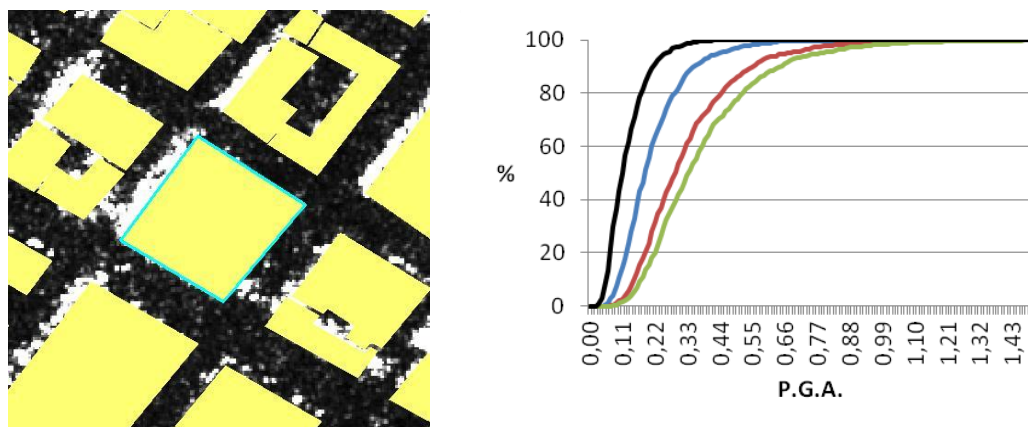
Fig. 6.2 An example of vulnerability study: The building under study (left), and its vulnerability curves (right)

Also in this case, SP-BELA was used in order to estimate the vulnerability of the structures, obtaining a results as in the Fig. 6.2. The y-axis represents the probability that the building reaching or exceeding a certain damage state, e.g. slight (black line), moderate (blue line), extensive (red line) and complete (green line), for a given level of Peak Ground Acceleration (PGA).

Starting from these results, it is possible to create a vulnerability map of the whole area under study. An example is reported in Fig. 6.3, where a vulnerability index has been assigned to every building; the results show three different classes, from low, to high probability to reach or exceed a certain damage state.

■	Low vulnerability
■	Moderate vulnerability
■	High vulnerability

Fig. 6.3 Example of vulnerability map for Messina

7   Closing Remarks

The report provides an insight into the potential of remote sensing for exposure mapping.

One finding of this study is that even in the high-income countries included in this study (Austria, Italy, and Greece) exposure and vulnerability data are not available with the information content and precision required for use in seismic loss assessment models at the municipality level. Aerial photography and, increasingly, high resolution remote sensing data - now widely available from commercial data providers – can be used to generate exposure data through visual analysis of the aerial or high resolution satellite imagery. Similarly, transport networks are typically extracted through digital encoding of information detected from imagery.

The methods for automatic extraction of <u>building parameters</u> from the imagery, addressed in this report, have not yet reached operational standards. However, techniques are improving, and automatically derived building stock may be available with high accuracy in the near future (Ehrlich *et al.*, 2012). Also, even the automatically derived building stock information aggregated over larger areas such as the 30 x 30 arc sec grids units used within the Global Exposure Database of the Global Earthquake Model (GEM, www.globalquakemodel.org) may prove to be sufficiently accurate. Population data is also not available for crisis management and this report shows examples of procedures to downscale population information available at coarse geographical units to the building level, based on building stock information derived from remote sensing. The procedures may prove to be of use also for continental population disaggregation, should a built up layer be available.

Aerial and High Resolution imagery mainly provide the geographical position, and when available the size and shape of the buildings that make up the building stock. A small number of building attributes can also be derived. For example, this report shows the example of extraction of the number of storeys in buildings in Thessaloniki. Disaster loss modellers should now assess the quality of this height assessment and its use within their models. The report also shows the importance of buildings spatial arrangement, shape, connectivity, essential for the systemic vulnerability assessment addressed in SYNER-G.

Many of the structural characteristics and the occupancy information – attributes of the buildings - that are needed to define the vulnerability of the building stock cannot be derived from imagery using automatic information extraction techniques. However, this report shows that some information can be derived from skilled photo-interpreters trained in civil engineering. Reliable structural information has to be collected from close visual inspection from the ground through field surveys and by civil engineers or trained experts. This report shows entry forms used to collect such information that can be embedded with hand-held technologies for rapid data gathering. The same hand-held technologies can be used to record occupancy and building use that are equally important for vulnerability assessment.

Building specific structural information together with remote sensing derived building stock inventory maps can then be combined within exposure/vulnerability databases that are structured as geographic information layers. The information should be structured based on European agreed standards. The structural information from field surveys – collected on a fraction of the total buildings on a city – can be extrapolated using the larger building stock that has been inventoried through satellite imagery. That data structured within a geographic

information layer can then become the data infrastructure from which disaster loss models can be executed.

The work of this report contributes to define the state-of-the-art in exposure and, to some extent, vulnerability assessment in Europe. Two important findings are the lack of available exposure and vulnerability, data and the lack of standardization/procedures for collection of exposure and vulnerability information for the three countries. This report shows examples on how remote sensing can be used to address the shortcomings. The report also contributes to define guidelines for use in the aforementioned Global Exposure Database (GED) of the Global Earthquake Model (GEM).

References

Ahola, T., K. Virrantaus, J. M. Krisp and G. J. Hunter, 2007. A spatio-temporal population model to support risk assessment and damage analysis for decision-making. *International Journal of Geographical Information Science* 21, 935-953.

Alberti, M., and P. Waddell. 2000. An integrated urban development and ecological simulation model. Integrated Assessment 1 (3): 215-227

Annunziato, A., S. Gadenz, D. Galliano, R. Guana and F. Igualada, 2010. Field tracking tool: a collaborative framework from the field to the decision makers, In: Konecny M., S. Zlatanova, T. L. Bandrova (Eds.),, *Geographic Information and Cartography for Risk and Crisis Management, Lecture Notes in Geoinformation and Cartography,* Springer Berlin Heidelberg, pp. 287-303.

Argyroudis, S., 2010. *Contribution to Seismic Vulnerability and Risk of Transportation Networks in Urban Environment*, PhD Thesis (in Greek), Dept. of Civil Engineering, Aristotle University of Thessaloniki, Greece.

Azar,D., J. Graesser, R. Engstrom, J. Comenetz, R.M. LeddyJr, N.G. Schechtman, T. Andrews. 2010.Spatial refinement of census population distribution using remotely sensed estimates of impervious surfaces in Haiti. International Journal of Remote Sensing, 31 (21): 5635–5655.

Baggio, C, A. Bernardini, R. Colozza, R. Corazza, M. Della Bella, G. Di Pasquale, M. Dolce, A. Goretti, A. Martinelli, G. Orsini, F. Papa and G. Zuccaro, 2007. *Field Manual for post-earthquake damage and safety assessment and short term countermeasures* (AeDES), Ed.s Pinto AV, Taucer F, Translation from Italian: Rota, M. and A. Goretti, European Communities.

Batista e Silva, F., F.J. Gallego. 2010. European Population Density Map 2006. Copenhagen (Denmark): European Environment Agency. JRC61399

Batista e Silva, F., C. Lavalle, and E. Koomen, 2012. A procedure to obtain a refined European land use/cover map. *Journal of Land Use Science*, in press.

Bhaduri, B., E. Bright, P. Coleman and M. Urban. 2007.LandScan USA: A High Resolution Geospatial and Temporal Modeling Approach for Population Distribution and Dynamics. *GeoJournal* 69: 103-117.

Borzi, B., H. Crowley, and R. Pinho, 2008 (a). Simplified Pushover-Based Vulnerability Analysis for Large Scale Assessment of RC Buildings. *Engineering Structures*. 30 (3): 804-820.

Borzi, B., H. Crowley and R. Pinho, 2008(b). Simplified Pushover-Based Earthquake Loss Assessment (SP-BELA) Method for Masonry Buildings. *International Journal of Architectural Heritage*, 2(4): 353 — 376.

Briggs, D. J., J. Gulliver, D. Fecht, D. M. Vienneau. 2007. Dasymetric modelling of small-area population distribution using land cover and light emissions data. *Remote Sensing of Environment* 108 (2007): 451–466.

Brunner, D., G. Lemoine, and L. Bruzzone. 2010. Earthquake Damage Assessment of Buildings Using VHR Optical and SAR Imagery. *IEEE Transactions On Geoscience And Remote Sensing* 48 (5).

Cai, Q., G.Rushton, B.Bhaduri, E. Bright, and P. Coleman. 2006. Estimating Small-Area Populations by Age and Sex Using Spatial Interpolation and Statistical Inference Methods. Transactions in GIS, 10(4): 577–598.

Chen, K., 2002. An approach to linking remotely sensed data and areal census data. *International Journal of Remote Sensing*,23(1): 37–48.

Dell'Acqua, F, P. Gamba, and G. Lisini, 2005. *Urban land cover mapping using hyperspectral and multispectral vhr Sensors: spatial versus spectral resolution*. In: Proceedings of the ISPRS Joint Symposium URBAN05 and URS05, Tempe, AZ, USA, March 14-16 2005.

Dell'Acqua, F, 2008. The role of SAR Sensors. In Global Mapping of Human Settlement. In: P. Gamba and M. Herlod Eds. Taylor and Fracis Series, *Remote Sensing Applications*, CRC Press, pp. 309-319.

Dell'Acqua, F., P. Gamba, and D. A. Polli, 2011. *Earthquake damage assessment from post-event VHR radar data: from Sichuan*, 2008 to Haiti, 2010. In: STilla, U. Gamba, Jurgens C., Maktav D (eds), JURSE 2011 – Joint Urban Remote Sensing Event, Munich, Germany, April 11-13, 2011.

Dell'Acqua, F., D. A. Polli, P. Tenerelli and D. Ehrlich., 2011. *D2.14 - Methods to extract building and road infrastructures from remote sensing and integration with ancillary information*. SYNER-G Deliverable Report.

Dobson, J., E. Bright, P. Coleman, R. Durfee and B. Worley. 2000. LandScan: A global population database for estimating populations at risk. *Photogrammetric Engineering and Remote Sensing*, Volume: 66, Issue: 7, Publisher: Taylor & Francis, Pages: 849-857

Dong, P., S. Ramesh, and A. Nepali. 2010.Evaluation of small-area population estimation using LiDAR, Landsat TM and parcel data. International Journal of Remote Sensing 31 (21): 5571–5586.

EEA, 1999. *CORINE Land Cover*. Brussels, Belgium.

EEA, 2010. *GMES Urban Atlas*. http://www.eea.europa.eu/data-and-maps/data/urban-atlas/ Last accessed on 10 Jan 2012.

Ehrlich D. and P. Tenerelli, 2012. Optical satellite imagery for quantifying spatio-temporal dimension of physical exposure in disaster risk assessments. *Natural Hazards.* Submitted.

Eicher, C., and C. Brewer. 2001. Dasymetric mapping and areal interpolation: implementation and evaluation. *Cartography and Geographic Information Science* 28: 125–138.

EUROSTAT, 1997. *Classification of Types of* Constructions (CC).

FEMA, 2002. *Rapid visual screening of buildings for potential seismic hazards: a handbook.* Washington, DC: Federal Emergency Management Agency; FEMA-154.

Franchin, P., F. Cavalieri, P.E. Pinto, et al., 2011. *Deliverable 2.1-General methodology for systemic seismic vulnerability assessment*, SYNER-G Project.

Gallego, F.J., 2010. A population density grid of the European Union. *Population and Environment*. 31: 460-473.

Gallego, F.J., F. Batista, C.Rocha, and S. Mubareka.2011. Disaggregating population density of the European Union with CORINE Land Cover. *International Journal of Geographical Information Science*, in press.

Gamba, P., F. Dell'Acqua and G. Lisini, 2009. *BREC: the Built-up area RECognition tool*. Joint Urban Remote Sensing Event, 22-24 May 2009, Shanghai.

Gao, J., 2009. *Digital Analysis of Remotely Sensed Imagery.* McGraw-Hill, New York, 2009, 645.

Gueguen L., M. Pesaresi, A. Gerhardinger, P. Soille, 2011. Characterizing and Counting Roofless Buildings in Very High Resolution Optical Images journal IEEE Geoscience and Remote Sensing Letters November 27, 2011

Harvey,J. T. 2002. Estimating census district populations from satellite imagery: Some approaches and limitations. International Journal of Remote Sensing 23 (10): 2071-2095.

Herold, M., M.E. Gardner and D.A. Roberts, 2003. Spectral resolution requirements for mapping urban areas. *IEEE Trans. Geosc. Remote Sens*, 41(9): 1907-1919.

Holt, J., C.P. Lo, T. W. Hodler.2004. Dasymetric estimation of population density and areal interpolation of census data. Cartography and Geographic Information Science, 31: 103–121.

Jaiswal, K.S. and DJ. Wald, 2008. *Creating a global building inventory for earthquake loss assessment and risk management.* U.S. Geological Survey, Open File Report 2008-1160, USGS. p. 109.

Kappos, A.J., G. Panagopoulos and G. Penelis, 2008. Development of a Seismic Damage and Loss Scenario for Contemporary and Historical Buildings in Thessaloniki, Greece. *Soil Dynamics and Earthquake Engineering*, 28(10-11): 836-850.

Khazai, B., J. Braun, B. V. Vangelsten and S. Duzgun, 2011. *D2.10 Development of an innovative methodology to assess socio-economic losses based on indicators* , SYNER-G Project.

Legates, D. R., and G. J. Mccabe Jr., 1999. Evaluating the Use of "Goodness-of-Fit" Measures in Hydrologic and Hydroclimatic Model Validation, *Water Resources Research*, 35(1), 233–241.

Li,G., and Q. Weng. 2005. Using Landsat ETM Imagery to Measure Population Density in Indianapolis, Indiana, USA. Photogrammetric Engineering & Remote Sensing, 71 (8): 947–958.

Liu, X. and K. C. Clarke. 2002. Estimation of residential population using high resolution satellite imagery. In: Proceedings, Third International Symposium on Remote Sensing of Urban Areas, June 2002, Istanbul, Turkey, pp. 153-160.

Lu, D., Q. Weng, and G. Li. 2006. Residential population estimation using a remote sensing derived impervious surface approach. International Journal of Remote Sensing, 27 (16): 3553–3570.

Lu, Z. ,J. Im, L. Quackenbush, K. Halligan. 2010.Population estimation based on multi-sensor data fusion. *International Journal of Remote Sensing*, 31 (21): 5587–5604.

Marino, C.M., C. Panigada and L. Busetto, 2001. *Airborne hyperspectral remote sensing applications in urban areas: asbestos concrete sheeting identification and mapping.* In: Proc. of the 1st IEEE/ISPRS Joint Workshop on Remote Sensing and Data Fusion over Urban Areas, Rome, Italy, 8-9 Nov. 2001, pp. 212-216.

Martin, D., S. Cockings, and S. Leung. 2009. *Population 24/7: building time-specific population grid models.* In European Forum for Geostatistics Conference 2009, The Hague, Netherlands, 5-7 October 2009.

McGarigal, K., and B.J. Marks., 1995. *FRAGSTATS: Spatial pattern analysis program for quantifying landscape structure.* Corvallis: Forest Science Department, Oregon State University.

Mennis, J., 2003. Generating surface models of population using dasymetric mapping. *The Professional Geographer*, 55: 31–42.

Mennis, J. and Hultgren, T., 2006. Intelligent dasymetric mapping and its application to areal interpolation. *Cartography and Geographic Information Science*, 33(3): 179-194.

Miura, H., S. Midorikawa, and FujimotoK., 2004. *Automated building detection from High-resolution satellite image for updating GIS building inventory data*. In: 13th World Conference on Earthquake Engineering Vancouver, B.C., Canada, August 1-6, 2004.

Miura, H., and S. Midorikawa. 2006. Updating GIS Building Inventory Data Using High-Resolution Satellite Images for Earthquake Damage Assessment: Application to Metro Manila, Philippines. *Earthquake Spectra*, 22 (1): 151-168.

Mueller, M, K, Segl, U, Heiden, H. Kaufmann, 2006. Potential of High-Resolution Satellite Data in the Context of Vulnerability of Buildings. *Natural Hazards* 38:247-258.

McLane, T. R. and K. and A. Porter, 2008. *ROVER - Rapid Observation of Vulnerability and Estimation of Risk*. http:// www.sparisk.com/pubs/McLane-Porter-02-Aug-2008-ROVER-overview.pdf.

Mrozinski, R.D., and R. Cromley. 1999. Singly-and doubly-constrained methods of areal interpolation for vector-based GIS. Transactions in Geographical Information Systems, 3: 285–301.

Nolte, E.M., B. Khazi and F. Wenzel. 2011. *D2.16 Vulnerability assessment by optical satellite Imagery.* SYNER-G Deliverable Report.

Noronha, S., and R. Nevatia. 2001. Detection and Modeling of Buildings from Multiple Aerial Images. *IEEE Transactions On Pattern Analysis And Machine Intelligence*, 23 (5).

O'Neil, R.V., B.T Milne., M.G. Turner, R.H. Gadner. 1988. *Resource utilization scales and landscape pattern.* Landscape Ecology. 2, pp 63-69*.*

Ouzounis, G.K., and P. Soille, 2010*. Differential Area Profiles. In: 20th International Conference on Pattern Recognition, 23-26 august 2010, Istanbul, Turkey*

Ouzounis, G.K., and P. Soille, 2011. *Attribute Constrained Connectivity and Alpha Tree Representation. IEEE Trans. Image Analysis. Submitted.*

Penelis, G.G., D. Sarigiannis, E. Stavrakakis and KC. Stylianidis, 1988. *A statistical evaluation of damage to buildings in the Thessaloniki, Greece, earthquake of June, 20, 1978*, Proceedings of the 9th World Conf. on Earthq. Engng., Tokyo-Kyoto, Japan, Aug. 1988, Tokyo: Maruzen, VII:187-192.

Persaresi, M. and J. A. Benediktsson, 2001. A new approach for the morphological segmentation of high resolution satellite imagery. *IEEE Transactions on Geoscience and Remote Sensing*, 39(2):309–320.

Pesaresi, M., A. Gerhardinger, and F. Kayitakire. 2008. A robust built-up area presence index by anisotropic rotation-invariant textural measure. *IEEE Journal of Selected Topics in Applied Earth Observations and Remote Sensing*, 1 (3): 180-192.

Pesaresi M, G.K. Ouzounis, and L. Gueguen. 2012. *A new compact representation of morphological profiles: report on first massive VHR image processing at the JRC*. Proc. SPIE 8390, 839025.

Poli, D., Angiuli E. and Remondino F., 2010. Radiometric and geometric analysis of WorldView-2 stereo scenes. *International Archives of Photogrammetry and Remote Sensing and Spatial Information Sciences*, Vol. XXXVIII, Part 1, 15-18 June 2010, Calgary, Canada.

Potere, D. and A. Schneider, 2009. Comparison of global urban maps. In: *Global Mapping of Human Settlements,* Ed. P. Gamba and M Herlod, CRC Press, 2009, pp. 269-308.

Schneiderbauer, S., and D. Ehrlich. 2005. Population density estimations for disaster management. Case study rural Zimbabwe. In: van Oosterom, P., S.Zlatanova, E.M. Fendel.Geo-information for Disaster Management. Proc. of the 1st International Symposium on Geo-information for Disaster Management', Delft, The Netherlands, March 21-23, 2005. Eds. Springer, 901-922.

Shao, Y., G.N. Taff, S.J. Walsh, 2011. Shadow detection and building height estimation using IKONOS data. *International Journal of Remote Sensing*, 32 (22): 6929-6944.

Schnedier, A., M. Friedl, and D. Potere, 2009. A new map of global urban extent from MODIS remote sensing data based on an urban ecoregion approach. In: *Global Mapping of Human Settlements*, Ed. P. Gamba and M Herlod, CRC Press, 2009, pp. 107-125.

Silván-Cárdenas, J. L., L. Wang, P.Rogerson, C.Wu, T.Feng and B.D.Kamphaus, 2010. Assessing fine-spatial-resolution remote sensing for small-area population estimation. *International Journal of Remote Sensing*, 31 (21): 5605–5634.

Soille, P. and M. Pesaresi, 2011. *Morphological Image Analysis for Remote Sensing City Analysis*. In: Remote Sensing City Analysis Workshop, Joint Research Centre, Ispra, 15-17 February, 2011.

Steinnocher, K., M. Köstl, J. Weichselbaum. 2011. Grid-based population and land take trend indicators. In Conference New Techniques and Technologies for Statistics –NTTS, 2011 Brussels, February 22-24.

SYNER-G, 2010a. *Working Document WD24*,SYNER-G project.

SYNER-G, 2010b. *Working Document WD21*, SYNER-G project.

Taubenböck, H., T. Esch, M. Wurm, A. Roth, and S. Dech. 2011. Object-based feature extraction using high spatial resolution satellite data of urban areas. Journal of Spatial Science, 55 (1): 117–132.

Taubenböck, H., T. Esch, A. Felbier, M. Wiesner, A. Roth, S. Dech, 2012. Monitoring urbanization in mega cities from space. *Remote Sensing of Environment*, 117 (15): 162-176.

Tenerelli, P., and D. Ehrlich. 2010. Analysis of built-up spatial pattern at different scales: can scattering affect map accuracy? International Journal of Digital Earth, in press, DOI: 10.1080/17538947.2010.512431

Tobler, W. R. 1979. Smooth pycnophylactic interpolation for geographical regions. Journal of the American Statistical Association, 74,367:519-530.

Toutin, TH, 2004a. DSM generation and evaluation from QuickBird stereo imagery with 3D physical modelling. *International Journal of Remote Sensing*, 25(22): 5181-5193.

Toutin, T.H., 2004b. Comparison of Stereo-Extracted DTM from Different High-Resolution Sensors: SPOT-5, EROS-A, IKONOS-II, and QuickBird. *IEEE Transactions on Geoscience and Remote Sensing*, 42(10): 2121-2129.

Toutin, T.H., 2006a. Comparison of DSMs Generated from Stereo HR Images Using 3D Physical or Empirical Models. *Photogrammetric Engineering and Remote Sensing*, 72 (5): 597-60.

Toutin, T.H., 2006b. Generation of DSM from SPOT-5 in-track HRS and across-track HRG stereo data using spatiotriangulation and autocalibration. *ISPRS Journal of Photogrammetry and Remote Sensing*, 60 (3): 170-181.

Vogelmann, J.E., S.M. Howard, L. Yang, C.R. Larson, B.K. Wylie, and J.N. Van Driel, 2001. Completion of the 1990's National Land Cover Data Set for the conterminous United States. *Photogrammetric Engineering and Remote Sensing*, 67:650-662.

Wieland, M., M. Pittore, S. Parolai, J. Szchau, B. Moldobekov and U. Begaliev, 2012. Estimating building inventory for rapid seismic vulnerability assessment: Towards an integrated approach based on multi-source imaging. *Soil Dynamics and Earthquake Engineering* 36:78-83.

Willmott, C. J., and Matsuura, K., 2005. Advantages of the mean absolute error (MAE) over the root mean square error (RMSE) in assessing average model performance. *Climate Research*, 30(1), 79-82.

Wu,C., and A.T. Murray. 2007. Population Estimation Using Landsat Enhanced Thematic Mapper Imagery. Geographical Analysis 39: 26–43.

Wu,S.S., Qiu,X., and Wang,L.. 2006. Using Semi-variance Image Texture Statistics to Model Population Densities. *Cartography and Geographic Information Science* (33) 2: 127-140.

Wu,S.S., L. Wang, and X. Qiu. 2008.Incorporating GIS Building Data and Census Housing Statistics for Sub-Block-Level Population Estimation. The Professional Geographer, 6(1): 121–135

Xi,F., H.S. He, Y. Hu, X. Wu, R. Bu, Y. Chang, M. Liu, and J. Yu. 2009. Simulate urban growth based on RS, GIS, and SLEUTH model in Shenyang-Fushun metropolitan area northeaster China. In: Urban Remote Sensing Event, 2009 Joint,20-22 May 2009, Shanghai.

Yuan, Y., R. Smith, and W. Limp. 1997. Remodelling census population with spatial information from LandsatTM imagery. *Computers Environment and Urban Systems*, 21: 245–258.

Abstract

This report summarizes the lessons learnt in extracting exposure information for the three study sites, Thessaloniki, Vienna and Messina that were addressed in SYNER-G. Fine scale information on exposed elements that for SYNER-G include buildings, civil engineering works and population, is one of the variables used to quantify risk. Collecting data and creating exposure inventories is a very time-demanding job and all possible data-gathering techniques should be used to address the data shortcoming problem. This report focuses on combining direct observation and remote sensing data for the development of exposure models for seismic risk assessment. In this report a summary of the methods for collecting, processing and archiving inventory datasets is provided in Chapter 2. Chapter 3 deals with the integration of different data sources for optimum inventory datasets, whilst Chapters 4, 5 and 6 provide some case studies where combinations between direct observation and remote sensing have been used. The cities of Vienna (Austria), Thessaloniki (Greece) and Messina (Italy) have been chosen to test the proposed approaches.

As the Commission's in-house science service, the Joint Research Centre's mission is to provide EU policies with independent, evidence-based scientific and technical support throughout the whole policy cycle.

Working in close cooperation with policy Directorates-General, the JRC addresses key societal challenges while stimulating innovation through developing new standards, methods and tools, and sharing and transferring its know-how to the Member States and international community.

Key policy areas include: environment and climate change; energy and transport; agriculture and food security; health and consumer protection; information society and digital agenda; safety and security including nuclear; all supported through a cross-cutting and multi-disciplinary approach.

Publications Office